

Search for new physics in events with same-sign dileptons and jets in pp collisions at $\sqrt{s} = 8$ TeV

The CMS Collaboration*

Abstract

A search for new physics is performed based on events with jets and a pair of isolated, same-sign leptons. The results are obtained using a sample of proton-proton collision data collected by the CMS experiment at a centre-of-mass energy of 8 TeV at the LHC, corresponding to an integrated luminosity of 19.5 fb^{-1} . In order to be sensitive to a wide variety of possible signals beyond the standard model, multiple search regions defined by the missing transverse energy, the hadronic energy, the number of jets and b-quark jets, and the transverse momenta of the leptons in the events are considered. No excess above the standard model background expectation is observed and constraints are set on a number of models for new physics, as well as on the same-sign top-quark pair and quadruple-top-quark production cross sections. Information on event selection efficiencies is also provided, so that the results can be used to confront an even broader class of new physics models.

Published in the Journal of High Energy Physics as doi:10.1007/JHEP01(2014)163.

1 Introduction

In the standard model (SM), proton-proton collision events having a final state with isolated leptons of the same sign are extremely rare. Searches for anomalous production of same-sign dileptons can therefore be very sensitive to new physics processes that produce this signature copiously. These include supersymmetry (SUSY) [1–3], universal extra dimensions [4], pair production of $T_{5/3}$ particles (fermionic partners of the top quark) [5], heavy Majorana neutrinos [6], and same-sign top-quark pair production [7, 8]. In SUSY, for example, same-sign dileptons occur naturally with the production of gluino pairs, when each gluino decays to a top quark and a top anti-squark, with the anti-squark further decaying into a top anti-quark and a neutralino.

In this paper we describe searches for new physics with same-sign dileptons (ee , $e\mu$, and $\mu\mu$) and hadronic jets, with or without accompanying missing transverse energy (E_T^{miss}). Our choice of signatures is driven by the following considerations. New physics signals with large cross sections are likely to be produced by strong interactions, and we thus expect significant hadronic activity in conjunction with the two leptons. Astrophysical evidence for dark matter [9] suggests considering SUSY models with R -parity conservation, which provides an excellent dark matter candidate — a stable lightest supersymmetric particle (LSP) that escapes detection. Therefore, a search for this signature involves sizable E_T^{miss} due to undetected LSPs. Nevertheless, we also consider signatures without significant E_T^{miss} in order to be sensitive to SUSY models with R -parity violation (RPV) [10] which imply an unstable LSP. Beyond these general guiding principles, the choice of signatures is made independently of any particular physics model and, as a result, these signatures can be applied also to probe non-supersymmetric extensions of the SM.

The results reported in this document expand upon a previous search [11] and are based on the proton-proton collision dataset at $\sqrt{s} = 8$ TeV collected with the Compact Muon Solenoid (CMS) detector at the Large Hadron Collider (LHC) during 2012, corresponding to an integrated luminosity of 19.5 fb^{-1} . We consider several final states, characterized by the scalar sum (H_T) of the transverse momenta (p_T) of jets, E_T^{miss} , the number of jets, and the number of jets identified as originating from b quarks (b -tagged jets). Additionally, in order to provide coverage for a wide range of generic signatures, we perform the analysis with two different requirements on the lepton p_T : the high- p_T analysis, where the leptons are selected with a p_T requirement of at least 20 GeV, and the low- p_T analysis, where the p_T threshold is lowered to 10 GeV. While the low- p_T leptons extend the sensitivity to scenarios with a compressed spectrum of SUSY particle masses, the high- p_T analysis targets models where the leptons are produced via on-shell W or Z bosons, and is less subject to backgrounds with leptons originating from jets. The use of a lower threshold on lepton p_T for the low- p_T analysis is compensated by a tighter H_T requirement. In this respect, the two searches are complementary, even if partially overlapping.

In contrast to the previous analysis [11], the signal regions within each of the low- and high- p_T analyses are defined to be exclusive. Furthermore, we increase the number of search regions in order to improve the sensitivity to a wider class of beyond-standard-model (BSM) processes. The selection criteria for the analysis objects and the methods used to estimate the SM backgrounds are largely unchanged from those of our previous same-sign dilepton studies [11–14].

Tables of observed yields and estimated SM backgrounds are provided for both the high- p_T and low- p_T analyses in each exclusive signal region. Having found no evidence for a BSM contribution to the event counts, limits are set on a variety of SUSY-inspired models by performing a counting experiment in each exclusive search region. Additionally, results for the

high- p_T analysis are used to set upper limits on the cross sections of the same-sign top-quark pair production and quadruple top-quark production, which can arise from new physics or as rare processes in the SM.

Finally, we include additional information on the event selection efficiencies to facilitate the interpretation of these results within models not considered in this paper.

2 The CMS detector

The central feature of the CMS apparatus is a superconducting solenoid, of 6 m internal diameter, providing a magnetic field of 3.8 T. The experiment uses a right-handed coordinate system, with the origin defined to be the nominal interaction point, the x axis pointing to the centre of the LHC ring, the y axis pointing up, and the z axis pointing in the anticlockwise-beam direction. The polar angle θ is measured from the positive z axis and the azimuthal angle ϕ is measured in the x - y (transverse) plane. The pseudorapidity η is defined as $\eta = -\ln[\tan(\theta/2)]$. Within the magnetic field volume are a silicon pixel and strip tracker, a crystal electromagnetic calorimeter, and a brass-scintillator hadron calorimeter. Muons are measured in gas-ionization detectors embedded in the steel flux-return yoke. Full coverage is provided by the tracker, calorimeters, and muon detectors within $|\eta| < 2.4$. In addition to the barrel and endcap calorimeters up to $|\eta| = 3$, CMS has extensive forward calorimetry reaching $|\eta| \lesssim 5$. Events are selected by a two-stage trigger system: a hardware-based trigger (L1) followed by a software-based high-level trigger (HLT) running on the data acquisition computer farm. A more detailed description of the CMS apparatus can be found in Ref. [15].

3 Event selection and Monte Carlo simulation

Events used in this search are selected using two complementary online algorithms. The high- p_T analysis uses a set of dilepton triggers, requiring the first (second) highest- p_T lepton to have $p_T > 17$ (8) GeV at the HLT. The low- p_T analysis uses high-level triggers that employ a reduced p_T threshold on leptons, of 8 GeV, and looser lepton identification requirements, but apply an additional online selection of $H_T > 175$ GeV. The minimum lepton p_T , the lepton identification requirements, and the H_T selections that are imposed offline for these two analyses are driven by the trigger selections. The selection efficiencies of these triggers for events used in this analysis vary between 81% and 96% and are discussed in detail in Section 6.

Offline, events with at least two isolated same-sign leptons (ee , $e\mu$ or $\mu\mu$) and at least two jets are selected. The lepton pairs are required to have an invariant mass above 8 GeV and to be consistent with originating from the same collision vertex. The requirement on the transverse impact parameter, calculated with respect to the primary vertex, has been tightened to 100 (50) μm for electrons (muons) compared to the previous versions of this analysis. This selection further suppresses the backgrounds from two sources: non-prompt leptons from semi-leptonic decays of heavy-flavour quarks and lepton charge misidentification. The algorithms used to calculate the isolation of the leptons, reconstruct jets, identify b-tagged jets, as well as the jet-lepton separation requirements are identical to the ones described in Refs. [11, 12]. For the identification of b-quark jets we continue to use the medium operating point of the combined secondary vertex (CSV) algorithm [16], which is based on the combination of secondary-vertex reconstruction and track-based lifetime information. The treatment of the effects of multiple proton-proton interactions within the same LHC bunch-crossing (pileup) on jet energies [17] also remains unchanged. Unlike the previous analysis, there is no requirement on the number of b-tagged

jets when selecting events. This number is, however, used in the categorization of events into various signal regions.

Table 1: Kinematic and fiducial requirements on leptons and jets that are used to define the low- p_T (high- p_T) analysis.

Object	p_T (GeV)	$ \eta $
Electrons	$>10(20)$	<2.4 and $\notin [1.4442, 1.566]$
Muons	$>10(20)$	<2.4
Jets	>40	<2.4
b-tagged jets	>40	<2.4

Kinematic selections for jets, leptons, and b-tagged jets are summarized in Table 1. Events with a third lepton are rejected if the lepton forms an opposite-sign same-flavour pair with one of the first two leptons for which the invariant mass of the pair ($m_{\ell\ell}$) satisfies $m_{\ell\ell} < 12$ GeV ($p_T > 5$ GeV) or $76 < m_{\ell\ell} < 106$ GeV ($p_T > 10$ GeV). These requirements are designed to minimize backgrounds from processes with a low-mass bound state or $\gamma^* \rightarrow \ell^+\ell^-$ in the final state, as well as multiboson (WZ, ZZ, and triboson) production.

Monte Carlo (MC) simulations, which include pileup effects, are used to estimate some of the SM backgrounds (see Section 5), as well as to calculate the efficiency for various new physics scenarios. All SM background samples are generated with the MADGRAPH 5 [18] program and simulated using a GEANT4-based model [19] of the CMS detector. Signal samples are produced with MADGRAPH 5 using the CTEQ6L1 [20] parton distribution functions (PDF); up to two additional partons are present in the matrix element calculations. Version 6.424 of PYTHIA [21] is used to simulate parton showering and hadronization, as well as the decay of SUSY particles. A signal sample for an RPV model is produced with PYTHIA 6.424. For signal samples, the detector simulation is performed using the CMS fast simulation package [22]. Detailed cross checks are performed to ensure that the results obtained with fast simulation are in agreement with the ones obtained with GEANT-based detector simulation. Simulated events are processed with the same chain of reconstruction programs that is used for data.

4 Search strategy

The search is based on comparing the number of observed events with the expectation from SM processes in several signal regions (SR) that have different requirements on four discriminating variables: E_T^{miss} , H_T , the number of jets, and the number of b-tagged jets. We define two sets of signal regions: *baseline* and *final* SRs. The former set imposes looser selection requirements, thereby forming a sample of events where the contributions of signal events are expected to be negligible, that is used to validate methods that are employed to predict the background in the final SRs; the latter set is based on tighter selection requirements, making it sensitive to many BSM processes. The interpretation of the results, discussed in Section 8, is primarily based on the final SRs.

Search regions defined in bins of the number of jets and b-tagged jets provide broad coverage of strongly produced SUSY particles, including signatures with low hadronic activity as well as signatures involving third-generation squarks. Additionally, as SUSY models with a small mass splitting between the parent sparticle and the LSP may result in low E_T^{miss} , we also define search regions with a looser requirement on E_T^{miss} . The high- p_T search is ideal for BSM models with an on-shell W boson produced in a new-physics particle decay, but events with an off-

shell W boson can produce low- p_T leptons, which is why leptons with transverse momenta as low as 10 GeV are included in this study.

Table 2: Definition of the baseline signal regions for the three different requirements on the number of b-tagged jets ($N_{b\text{-jets}}$). N_{jets} refers to the number of jets in the event. The same naming scheme is used for both the low- and high- p_T analyses, which differ only in a looser requirement on H_T (in parentheses) for the high- p_T analysis.

H_T (GeV)	E_T^{miss} (GeV)	N_{jets}	$N_{b\text{-jets}}$	SR name
>250 (80)	>30 if $H_T < 500$ else >0	≥ 2	=0	BSR0
>250 (80)	>30 if $H_T < 500$ else >0	≥ 2	=1	BSR1
>250 (80)	>30 if $H_T < 500$ else >0	≥ 2	≥ 2	BSR2

We define the three baseline signal regions (BSR0, BSR1, and BSR2) for both the low- and high- p_T analyses, as described in Table 2. The event selection criteria are tightened and the granularity of the regions is increased to define the 24 final SRs described in Table 3 for the high- p_T analysis. For the low- p_T signal regions, the categories are equivalent to those of the high- p_T analysis, but the selection differs in the requirement on H_T and lepton p_T . The threshold on H_T is increased from 200 to 250 GeV in order to ensure 100% efficiency for the triggers used by the low- p_T event selection. All 24 signal regions are mutually exclusive and may therefore be statistically combined within either high- p_T or low- p_T analysis.

Table 3: Definition of the signal regions for the high- p_T analysis. The low- p_T analysis employs a tighter requirement $H_T > 250$ GeV and uses the same numbering scheme, in which the first digit in the name represents the requirement on the number of b-tagged jets for that search region, e.g. SR01, SR11, and SR21 correspond to SRs with $N_{b\text{-jets}}$ 0, 1, and ≥ 2 , respectively.

$N_{b\text{-jets}}$	E_T^{miss} (GeV)	N_{jets}	$H_T \in [200, 400]$ (GeV)	$H_T > 400$ (GeV)
= 0	50–120	2–3	SR01	SR02
		≥ 4	SR03	SR04
	>120	2–3	SR05	SR06
		≥ 4	SR07	SR08
= 1	50–120	2–3	SR11	SR12
		≥ 4	SR13	SR14
	>120	2–3	SR15	SR16
		≥ 4	SR17	SR18
≥ 2	50–120	2–3	SR21	SR22
		≥ 4	SR23	SR24
	>120	2–3	SR25	SR26
		≥ 4	SR27	SR28

Additional (overlapping) signal regions, listed in Table 4, are defined with no or loose E_T^{miss} requirements in order to provide better sensitivity to scenarios such as RPV SUSY models and same-sign top-quark pair production. These search regions are formed using events that satisfy high- p_T lepton selection and contain at least two jets. Because in RPV SUSY scenarios the LSP decays, mainly into detectable leptons and quarks, such events are not expected to have large E_T^{miss} , but they usually have substantial H_T . Thus, in search regions designed for such models, the E_T^{miss} requirement is removed completely, while a relatively high $H_T > 500$ GeV requirement is applied to reduce the level of SM background. These search regions are labelled as RPV0 and RPV2 for $N_{b\text{-jets}} \geq 0$ and ≥ 2 , respectively.

Same-sign top quark pair events in which the W bosons decay leptonically generally contain moderate E_T^{miss} , due to the accompanying neutrinos. Using events with $E_T^{\text{miss}} > 30 \text{ GeV}$, we form four signal regions, denoted SStop1, SStop2, SStop1++, and SStop2++, where “++” refers to the selection of only positively charged dilepton pairs. Note that in most new physics scenarios, $pp \rightarrow \bar{t}t$ is suppressed with respect to $pp \rightarrow tt$ because the PDF of the proton is dominated by quarks, rather than anti-quarks. For such scenarios, the SStop1++ and SStop2++ signal regions are expected to provide higher sensitivity.

Table 4: Signal regions that are used in the search for same-sign top-quark pair production and RPV SUSY processes.

N_{jets}	$N_{\text{b-jets}}$	E_T^{miss} (GeV)	H_T (GeV)	Lepton charge	SR name
≥ 2	≥ 0	> 0	> 500	++/--	RPV0
≥ 2	≥ 2	> 0	> 500	++/--	RPV2
≥ 2	$= 1$	> 30	> 80	++/--	SStop1
≥ 2	$= 1$	> 30	> 80	++ only	SStop1++
≥ 2	≥ 2	> 30	> 80	++/--	SStop2
≥ 2	≥ 2	> 30	> 80	++ only	SStop2++

5 Backgrounds

There are three main sources of SM background in this analysis, which are described below. More details on the methods used to estimate these backgrounds can be found in Refs. [12, 14].

- “Non-Prompt leptons”, i.e. leptons from heavy-flavour decays, misidentified hadrons, muons from light-meson decays in flight, or electrons from unidentified photon conversions. The background caused by these non-prompt leptons, which is dominated by $t\bar{t}$ and $W + \text{jets}$ processes, is estimated from a sample of events with at least one lepton that passes a loose selection but fails the full set of tight identification and isolation requirements described in Section 3. The background rate is obtained by scaling the number of events in this sample by a “tight-to-loose” ratio, i.e. the probability that a loosely identified non-prompt lepton also passes the full set of requirements. Various definitions of the loose lepton selection criteria are studied in detail, and combination of relaxed isolation and lepton-identification requirements is used. These probabilities are measured as a function of lepton p_T and η , as well as event kinematics, in control samples of QCD multijet events that are enriched in non-prompt leptons.
- Rare SM processes that yield same-sign leptons, mostly from $t\bar{t}W$, $t\bar{t}Z$, and diboson production. We also include the contribution from the SM Higgs boson produced in association with a vector boson or a pair of top quarks in this category of background. All these backgrounds are estimated from MC simulation. The event yields are corrected for several effects, summarized in Section 6, to account for the differences between object selection efficiencies in data and simulation.
- Charge misidentification, i.e. events with opposite-sign isolated leptons where the charge of one of the leptons is misidentified because of severe bremsstrahlung in the tracker material. This background, which is relevant only for electrons and is negligible for muons, is estimated by selecting opposite-sign ee or $e\mu$ events passing the full kinematic selection and then weighting them by the p_T - and η -dependent probability of electron charge misassignment. This probability, which varies between

10^{-4} and 10^{-5} , is obtained from simulation and is then validated with a control data sample of $Z \rightarrow ee$ events.

Backgrounds stemming from non-prompt leptons constitute the major contribution to the total background in most search regions. The rare SM processes dominate in the search regions with large numbers of b-tagged jets or high E_T^{miss} requirements. The contribution from charge misidentification is generally much smaller and stays below the few-percent level in all search regions.

The primary origin of the systematic uncertainty for the non-prompt lepton background estimate is differences between the QCD multijet sample, where the “tight-to-loose” ratio is determined, and the signal regions, where the method is applied, both for the event kinematics and for the relative rates of the various sources of non-prompt leptons. A systematic uncertainty also arises because $t\bar{t}$ and $W + \text{jets}$ events, the two dominant components of the non-prompt background, differ themselves in the event kinematics and relative importance of the various sources, making it difficult to define a “tight-to-loose” ratio that is equally appropriate for both components. Based on the variation between true and predicted background yields when the background estimation method is applied to simulation, the systematic uncertainty of the estimate is assessed at 50%. This systematic part is the dominant uncertainty in the non-prompt lepton background estimate in most signal regions. The statistical uncertainty in the method is driven by the number of events in the sideband regions, defined with relaxed lepton requirements, that are used to estimate the non-prompt lepton background. As the kinematic selections are tightened, the statistical uncertainty becomes more important, becoming comparable in size to the systematic uncertainty in the search regions with the tightest selections.

For the rare SM processes, the next-to-leading-order (NLO) production cross sections are used to normalize the MC predictions. The cross section values used for the most relevant processes, $t\bar{t}W$ and $t\bar{t}Z$, are 232 fb [23] and 208 fb [24, 25], respectively. Because these and other rare processes are simulated using leading order (LO) generators, the systematic uncertainty for the rare SM background accounts both for the theoretical uncertainty in the cross sections and for the non-uniformity of the ratio between the LO and NLO cross sections as a function of jet multiplicity, H_T , and E_T^{miss} [23]. The systematic uncertainties for each SM process that contributes to this background are assigned to be 50% and are considered to be 100% correlated across all signal regions.

The uncertainty associated with the charge-misidentification background estimate, which is estimated to be 30%, accounts for differences between data and simulation, and the limited momentum range of electrons probed in the control sample.

The total background in each search region is obtained by summing the yields from each of these background sources, and the total uncertainty is calculated by considering the individual uncertainties to be uncorrelated.

6 Efficiencies and associated uncertainties

The trigger efficiency is measured with data, using triggers that are orthogonal to those described in Section 3. The measured efficiencies are summarized in Table 5. Correction factors to take the trigger inefficiencies into account are applied to all acceptances calculated from MC simulation, for both signal and background samples. We assign a 6% uncertainty to these efficiencies, based on the statistical uncertainty of the measurement and deviations from the quoted numbers in Table 5 as a function of $|\eta|$ and p_T .

Table 5: Summary of the trigger selection efficiencies for low- and high- p_T analyses in each channel. The thresholds on $|\eta|$ and p_T correspond to the lower p_T lepton of the dilepton pair.

Channel	Low- p_T	High- p_T
ee, $p_T < 30$ GeV	0.93 ± 0.06	0.92 ± 0.05
ee, $p_T > 30$ GeV	0.93 ± 0.06	0.96 ± 0.06
$e\mu$	0.93 ± 0.06	0.93 ± 0.06
$\mu\mu$, $ \eta < 1$	0.94 ± 0.06	0.90 ± 0.05
$\mu\mu$, $1.0 < \eta < 2.4$	0.90 ± 0.05	0.81 ± 0.05

The offline lepton selection efficiencies in data and simulation are measured using Z-boson events to derive simulation-to-data correction factors. The correction factors applied to simulation are 90 (96)% for $p_T < 20$ GeV and 94 (98)% for $p_T > 20$ GeV for electrons (muons). The uncertainty of the total efficiency is 5% (3%) for electrons (muons) with $p_T > 15$ GeV, increasing to 10% (5%) for lower transverse momentum. An additional systematic uncertainty is assigned to account for potential mismodelling of the lepton isolation efficiency due to varying hadronic activity in signal events. This uncertainty is 3% for all leptons except muons with $p_T < 30$ GeV, for which it is 5%.

Another source of systematic uncertainty is associated with the jet energy scale correction. This systematic uncertainty varies between 5% and 2% in the p_T range 40–100 GeV for jets with $|\eta| < 2.4$ [26]. It is evaluated on a single-jet basis, and its effect is propagated to H_T , E_T^{miss} , the number of jets, and the number of b-tagged jets. The importance of these effects depends on the signal region and the model of new physics. In general, models with high hadronic activity and large E_T^{miss} are less affected by the uncertainty in the jet energy scale. In addition, there is a contribution to the total uncertainty arising from limited knowledge of the resolution of the jet energy, but this effect is generally of less importance than the contribution from the jet energy scale.

The b-tagging efficiency for b-quark jets with $|\eta| < 2.4$, measured in data using samples enriched in $t\bar{t}$ and muon-jet events, has a p_T -averaged value of 0.72. The false positive b-tagging probability for charm-quark jets is approximately 20%, while for jets originating from light-flavour quarks or gluons it is of the order of 1%. Correction factors, dependent on jet flavour and kinematics, are applied to simulated jets to account for the differences in the tagging efficiency in simulation with respect to data. The total uncertainty of the b-tagging efficiency is determined by simultaneously varying the efficiencies to tag a bottom, charm, or light quark up and down by their uncertainties [16]. The importance of this effect depends on the signal region and the model of new physics. In general, models with more than two b quarks in the final state are less affected by this uncertainty.

Additional uncertainties due to possible mismodelling of the pileup conditions or initial-state radiation (ISR) [27] are evaluated and found to be 5% and 3–15%, respectively. The uncertainty of the signal acceptance due to the PDF choice is found to be less than a few percent. Finally, there is a 2.6% uncertainty in the yield of events because of the uncertainty in the luminosity normalization [28].

A summary of the systematic uncertainties associated with the acceptance and signal efficiency for this analysis is provided in Table 6. While the uncertainties associated with the integrated luminosity, modelling of lepton selection, trigger efficiency, and pileup are taken to be constant across the parameter space of the new physics models considered in this paper, uncertainties arising from the remaining observables are estimated for each model separately on an event-

by-event basis by varying those observables within their uncertainties. The total uncertainty in the computed acceptance is in the 13–25% range. The figures in Table 6 are representative values for these uncertainties and do not characterize the results for extreme kinematic regions, such as those near the diagonal of the parameter space of the SUSY simplified models discussed in Section 8, where the particle mass spectra are compressed.

Table 6: Summary of representative systematic uncertainties for the considered signal models.

Source	%
Luminosity	2.6
Modelling of lepton selection (ID and isolation)	10
Modelling of trigger efficiency	6
Pileup modelling	5
Jet energy scale	1–10
Jet energy resolution	0–3
b-jet identification	2–10
ISR modelling	3–15
Total	13–25

7 Results

The distributions of E_T^{miss} versus H_T for events in the three baseline signal regions are shown in Fig. 1. The results are shown separately for the low- and high- p_T samples. The corresponding results for the four selection variables H_T , E_T^{miss} , N_{jets} , and $N_{\text{b-jets}}$ are shown in Fig. 2. For these latter results, the SM background prediction is also shown. There are no significant discrepancies observed between the observations and background predictions for any region.

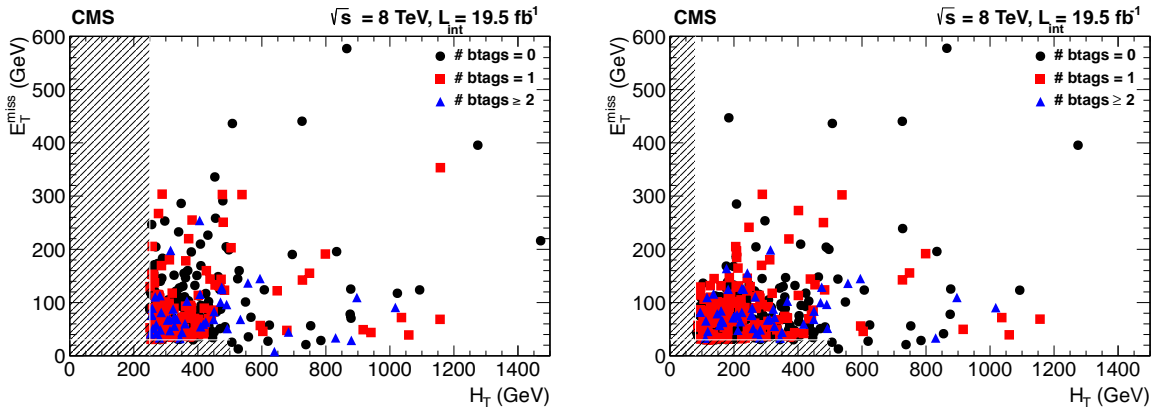


Figure 1: Distributions of E_T^{miss} versus H_T for the baseline signal regions BSR0, BSR1, and BSR2 for the low- p_T (left) and the high- p_T (right) analyses. The regions indicated with the hatched area are not included in the analyses.

The observations in each of the final signal regions are presented in Tables 7 and 8 and in Fig. 3 along with the corresponding SM background prediction. The contributions of rare SM processes and non-prompt leptons vary among the signal regions between 40% and 60%, while the charge misidentification background is almost negligible for all signal regions. The observations are consistent with the background expectations within their uncertainties. The p-

values [29] for each signal region in the low- and high- p_T analyses are studied, and are found to be consistent with a uniform distribution between 0 and 1.

Table 7: Predicted and observed event yields for the low- p_T and high- p_T signal regions.

Region	Low- p_T			High- p_T		
	Expected	Observed		Expected	Observed	
SR01	44 ± 16	50		51 ± 18	48	
SR02	12 ± 4	17		9.0 ± 3.5	11	
SR03	12 ± 5	13		8.0 ± 3.1	5	
SR04	9.1 ± 3.4	4		5.6 ± 2.1	2	
SR05	21 ± 8	22		20 ± 7	12	
SR06	13 ± 5	18		9 ± 4	11	
SR07	3.5 ± 1.4	2		2.4 ± 1.0	1	
SR08	5.8 ± 2.1	4		3.6 ± 1.5	3	
SR11	32 ± 13	40		36 ± 14	29	
SR12	6.0 ± 2.2	5		3.8 ± 1.4	5	
SR13	17 ± 7	15		10 ± 4	6	
SR14	10 ± 4	6		5.9 ± 2.2	2	
SR15	13 ± 5	9		11 ± 4	11	
SR16	5.5 ± 2.0	5		3.9 ± 1.5	2	
SR17	4.2 ± 1.6	3		2.8 ± 1.1	3	
SR18	6.8 ± 2.5	11		4.0 ± 1.5	7	
SR21	7.6 ± 2.8	10		7.1 ± 2.5	12	
SR22	1.5 ± 0.7	1		1.0 ± 0.5	1	
SR23	7.1 ± 2.7	6		3.8 ± 1.4	3	
SR24	4.4 ± 1.7	11		2.8 ± 1.2	7	
SR25	2.8 ± 1.1	1		2.9 ± 1.1	4	
SR26	1.3 ± 0.6	2		0.8 ± 0.5	1	
SR27	1.8 ± 0.8	0		1.2 ± 0.6	0	
SR28	3.4 ± 1.3	3		2.2 ± 1.0	2	

Table 8: Predicted and observed event yields in the signal regions designed for same-sign top-quark pair production and RPV SUSY models.

SR	Expected	Observed
RPV0	38 ± 14	35
RPV2	5.3 ± 2.1	5
SStop1	160 ± 59	152
SStop1++	90 ± 32	92
SStop2	40 ± 13	52
SStop2++	22 ± 8	25

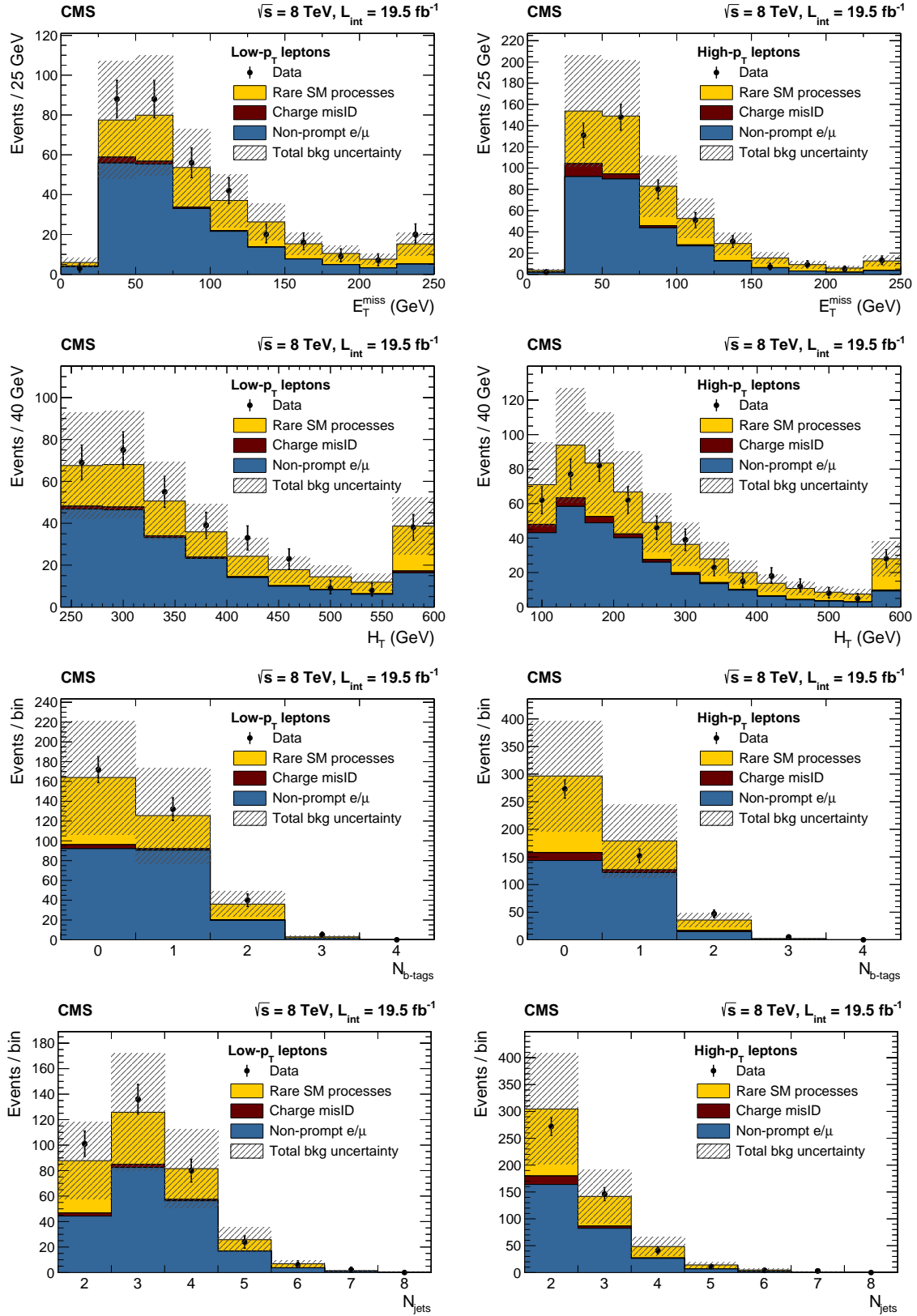


Figure 2: Distributions of E_T^{miss} , H_T , number of b-tagged jets, and number of jets for the events in the low- p_T (high- p_T) baseline region with no $N_{b\text{-jets}}$ requirement (events selected in BSR0, BSR1, and BSR2) are shown on the left (right). Also shown as a histogram is the background prediction. The shaded region represents the total background uncertainty.

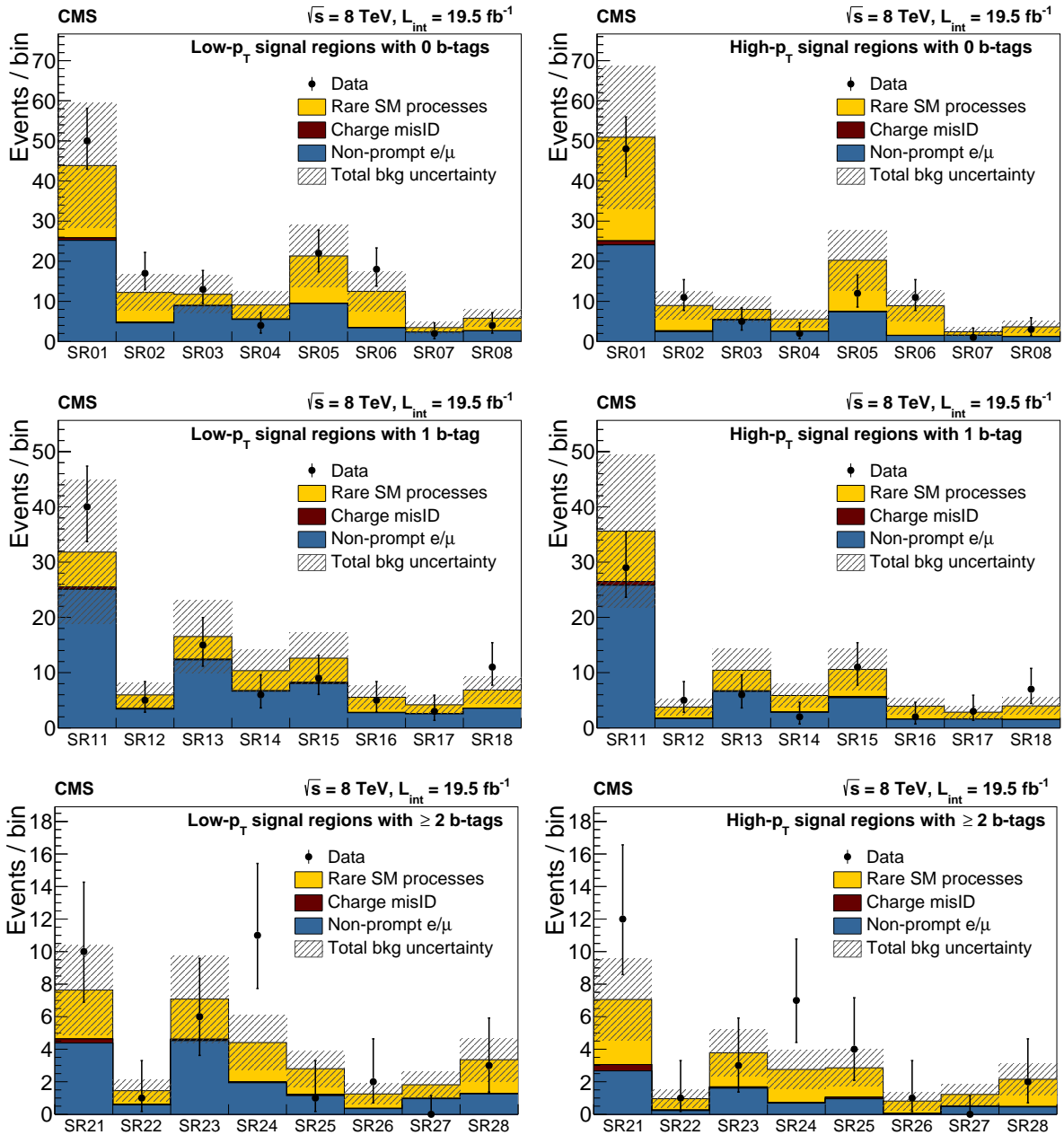


Figure 3: Summary plots showing the predicted background from each source and observed event yields as a function of the SRs in the low- p_T (high- p_T) analysis on left (right).

8 Limits on models of new physics and on rare SM processes

Given the lack of a significant excess over the expected SM background, the results of the search are used to derive limits on the parameters of various models of new physics and to derive limits on the cross sections of rare SM processes. The 95% confidence level (CL) upper limits on the signal yields are calculated using the LHC-type CL_s method [30–32]. Lognormal nuisance parameters are used for the signal (Table 6) and background estimate (Tables 7 and 8) uncertainties. For each model considered, limits are obtained by performing a statistical combination of the most sensitive signal regions.

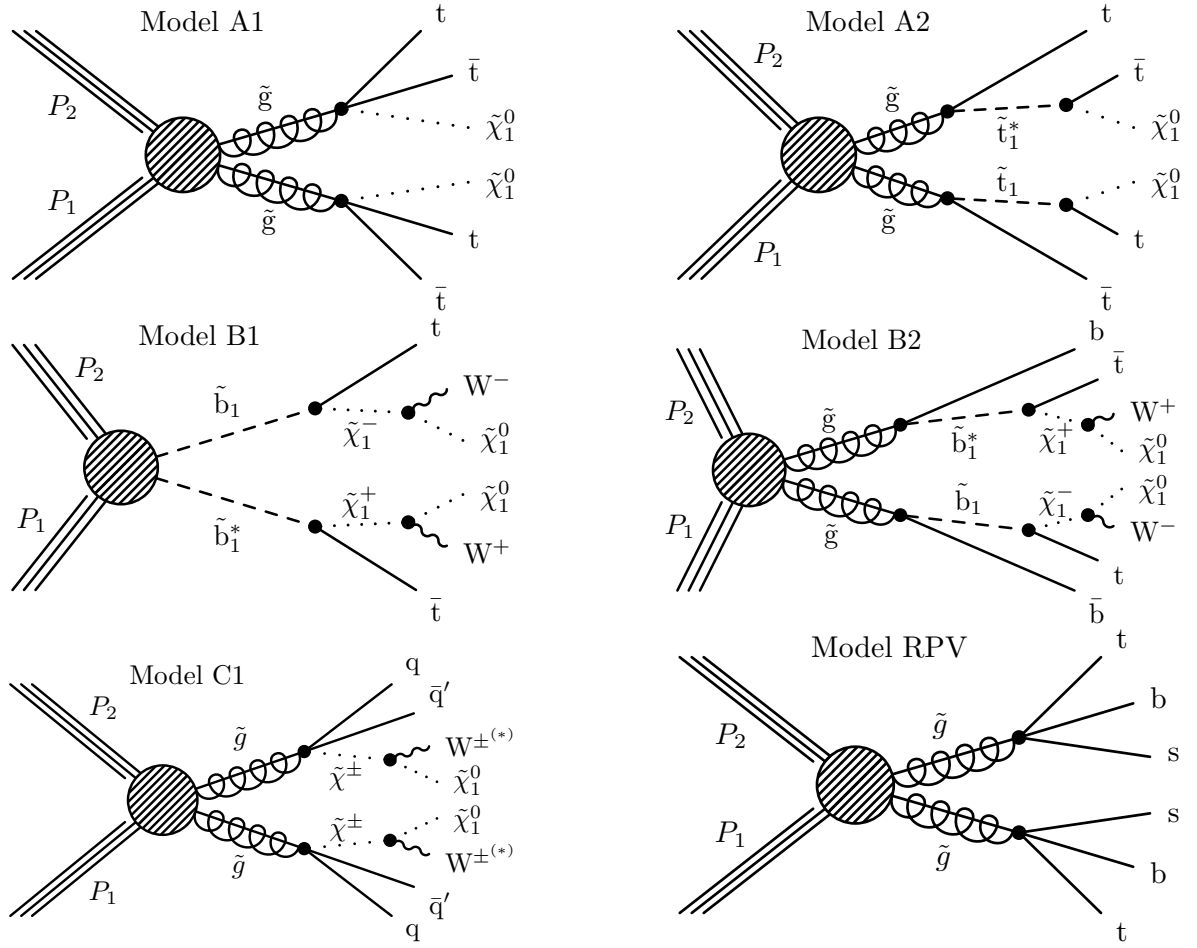


Figure 4: Diagrams for the six SUSY models considered (A1, A2, B1, B2, C1, and RPV).

The signal regions used to set limits on the new physics models explored in this paper are given in Table 9.

The number of events that are expected to satisfy the selection for a given signal model is obtained from MC simulation. The uncertainties for the event yields are computed as described in Section 6. For a given signal region, the different sources of uncertainties in the signal acceptance are considered to be uncorrelated, with correlations across signal regions taken into account. The uncertainties in the total background across the signal regions are considered to be fully correlated.

First, we present limits on the parameter spaces of various R -parity-conserving simplified SUSY models [33]. The exclusion contours are obtained with the gluino or bottom-squark pair production cross sections at the NLO+NLL (i.e. next-to-leading-logarithm) accuracy that are calculated in the limit where other sparticles are heavy enough to be decoupled [34–39]. The production of SUSY particles and the decay chains under consideration are shown schematically in Fig. 4.

Scenarios A1 and A2 represent models of gluino pair production resulting in the $t\bar{t}t\bar{t}\tilde{\chi}_1^0\tilde{\chi}_1^0$ final state, where $\tilde{\chi}_1^0$ is the lightest neutralino [33, 40–43]. In model A1, the gluino undergoes a three-body decay $\tilde{g} \rightarrow t\bar{t}\tilde{\chi}_1^0$ mediated by an off-shell top squark. In model A2, the gluino decays to a top quark and a top anti-squark, with the on-shell anti-squark further decaying into a top anti-quark and a neutralino. Both of these models produce four on-shell W bosons and four

Table 9: Signal regions used for limit setting for the new physics models considered in this analysis.

Model	Constraints on parameters	Analysis	Signal regions used
A1		high- p_T	21–28
A2	$m_{\tilde{\chi}_1^0} = 50 \text{ GeV}$	high- p_T	21–28
B1	$m_{\tilde{\chi}_1^0} = 50 \text{ GeV}$	high- p_T	11–18, 21–28
B1	$m_{\tilde{\chi}_1^0}/m_{\tilde{\chi}_1^\pm} = 0.5$	high- p_T	11–18, 21–28
B1	$m_{\tilde{\chi}_1^0}/m_{\tilde{\chi}_1^\pm} = 0.8$	low- p_T	11–18, 21–28
B2	$m_{\tilde{\chi}_1^0} = 50 \text{ GeV}, m_{\tilde{\chi}_1^\pm} = 150 \text{ GeV}$	high- p_T	21–28
B2	$m_{\tilde{\chi}_1^0} = 50 \text{ GeV}, m_{\tilde{\chi}_1^\pm} = 300 \text{ GeV}$	high- p_T	21–28
C1	$m_{\tilde{\chi}_1^\pm} = 0.5m_{\tilde{\chi}_1^0} + 0.5m_{\tilde{g}}$	high- p_T	01–08
C1	$m_{\tilde{\chi}_1^\pm} = 0.8m_{\tilde{\chi}_1^0} + 0.2m_{\tilde{g}}$	low- p_T	01–08
RPV		high- p_T	RPV2
pp \rightarrow tt, $\bar{t}\bar{t}$		high- p_T	SStop1, SStop2
pp \rightarrow tt		high- p_T	SStop1++, SStop2++
pp \rightarrow tt $\bar{t}\bar{t}$		high- p_T	21–28

b quarks. Therefore, search regions SR21–SR28, which require at least two b-tagged jets and high- p_T leptons, are used to derive the limits on the parameters of these models; the region with the best sensitivity is SR28. The 95% CL upper limits on the cross section times branching fraction, as well as the exclusion contours, are shown in Fig. 5. For model A1, the results are presented as a function of gluino mass and $\tilde{\chi}_1^0$ mass, and for model A2 as a function of gluino mass and top squark mass with the $\tilde{\chi}_1^0$ mass set to 50 GeV. In model A2, the limits do not depend on the top squark or $\tilde{\chi}_1^0$ masses provided that there is sufficient phase space to produce on-shell top quarks with a moderate boost in the decay of both the gluino and the top squark. This range extends to approximately 600 GeV for the $\tilde{\chi}_1^0$ mass.

Model B1 is a model of bottom-squark pair production, followed by one of the most likely decay modes of the bottom squark, $\tilde{b}_1 \rightarrow t\tilde{\chi}_1^-$ with $\tilde{\chi}_1^- \rightarrow W^- \tilde{\chi}_1^0$, where \tilde{b}_1 and $\tilde{\chi}_1^-$ represent the lightest bottom squark and lightest chargino, respectively. We consider three cases in this decay mode. We either set the $\tilde{\chi}_1^0$ mass to 50 GeV and present the limits in the $(m_{\tilde{\chi}_1^\pm}, m_{\tilde{b}_1})$ plane, or consider the $(m_{\tilde{\chi}_1^0}, m_{\tilde{b}_1})$ plane with the mass of the chargino set according to $m_{\tilde{\chi}_1^0}/m_{\tilde{\chi}_1^\pm} = 0.5$ or $m_{\tilde{\chi}_1^0}/m_{\tilde{\chi}_1^\pm} = 0.8$. The values 0.5 and 0.8 are representative choices that determine whether the top quark and W boson are on-shell or off-shell, which has a direct impact on the sensitivity of the analysis in this model. The limits for this model, obtained using search regions SR11 to SR28, are presented in Fig. 6. For $m_{\tilde{\chi}_1^0}/m_{\tilde{\chi}_1^\pm} = 0.8$, the low- p_T lepton selection is used, while high- p_T leptons are used for the other two scenarios. SR28 is again the most sensitive signal region, followed by the regions requiring one b-tagged jet: SR18, SR15, and SR13.

Model B2 consists of gluino pair production followed by $\tilde{g} \rightarrow \tilde{b}_1\bar{b}$. The gluino decay modes in models A1 and A2 are expected to be dominant if the top squark is the lightest squark. Conversely, if the bottom squark is the lightest, the decay mode in model B2 would be the most probable. The limits on this model, calculated using search regions SR21–SR28 and the high- p_T lepton selection, are presented in Fig. 6 as a function of $m(\tilde{b}_1)$ and $m(\tilde{g})$ for two fixed masses of $m_{\tilde{\chi}_1^\pm}$, 150 and 300 GeV. The region with the largest sensitivity to this model is SR28.

Model C1 is based on the production of a gluino pair where each gluino decays to light quarks

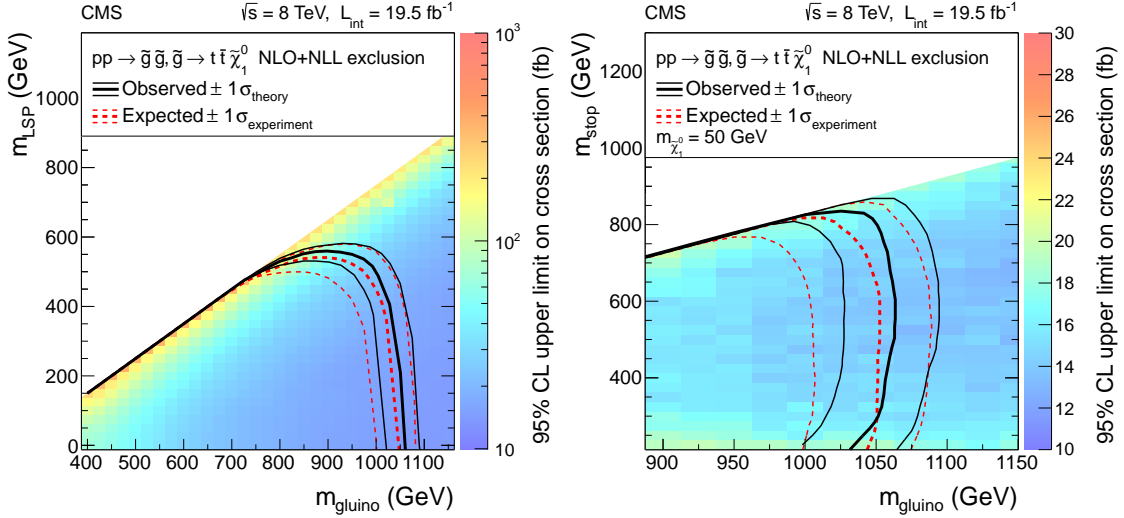


Figure 5: Exclusion regions at 95% CL in the planes of (left) $m(\tilde{\chi}_1^0)$ versus $m(\tilde{g})$ (model A1), and (right) $m(\tilde{t}_1)$ versus $m(\tilde{g})$ (model A2). The excluded regions are those within the kinematic boundaries and to the left of the curves. The effects of the theoretical uncertainties in the NLO+NLL calculations of the production cross sections [39] are indicated by the thin black curves; the expected limits and their ± 1 standard-deviation variations are shown by the dashed red curves.

and a chargino via heavy virtual squarks: $\tilde{g} \rightarrow q\bar{q}'\tilde{\chi}_1^\pm$, $\tilde{\chi}_1^\pm \rightarrow W^{(*)}\tilde{\chi}_1^0$. The decay is charge-symmetric, resulting in an equal fraction of same-sign and opposite-sign W boson pairs in the final state. In this model there are three parameters: $m_{\tilde{g}}$, $m_{\tilde{\chi}_1^\pm}$, and $m_{\tilde{\chi}_1^0}$. Signal samples are produced for each bin in the $(m_{\tilde{\chi}_1^0}, m_{\tilde{g}})$ plane. Chargino mass is defined through a parameter x as $m_{\tilde{\chi}_1^\pm} = xm_{\tilde{\chi}_1^0} + (1-x)m_{\tilde{g}}$. In the limit $x \rightarrow 0$, there is no observable hadronic activity in the event. At the other extreme, $x \rightarrow 1$, the chargino and LSP are degenerate and the chargino decays through an off-shell W boson yielding very soft leptons. In either cases, the analysis loses sensitivity. For intermediate values of the parameter x , the W boson is either on- or off-shell depending on the values of $m_{\tilde{\chi}_1^0}$ and $m_{\tilde{g}}$, giving rise to either high- or low- p_T leptons. We examine x values of 0.5 and 0.8. The former value ensures that the W boson is on-shell in the sparticle mass range considered, while the latter yields mostly off-shell W bosons. In this model, no enrichment of heavy-flavour jets is expected. Therefore, the search regions SR01–SR08, with both the low- and high- p_T lepton selection, are used for cross section upper limit calculation. The limits are presented in Fig. 7. In this model, gluino masses up to 900 GeV are probed. Most of the sensitivity to this model is obtained from signal region SR08.

These results extend the sensitivity obtained in the previous analysis [11] on gluino and sbottom masses. For the gluino-initiated models (A1, A2, B2, and C1), we probe gluinos with masses up to about 1050 GeV, with relatively small dependence on the details of the models. This is because the limits are driven by the common gluino pair production cross section. In the case of the direct bottom-squark pair production, model B1, our search shows sensitivity for bottom-squark masses up to about 500 GeV.

These models are also probed by other CMS new physics searches in different decay modes. Other searches are usually interpreted in the context of model A1 but not A2, B1, or B2. For model A1, the limits given here are complementary to the limits from the searches presented in Refs. [44–47]. In particular, they are less stringent at low $m(\tilde{\chi}_1^0)$ but more stringent at high

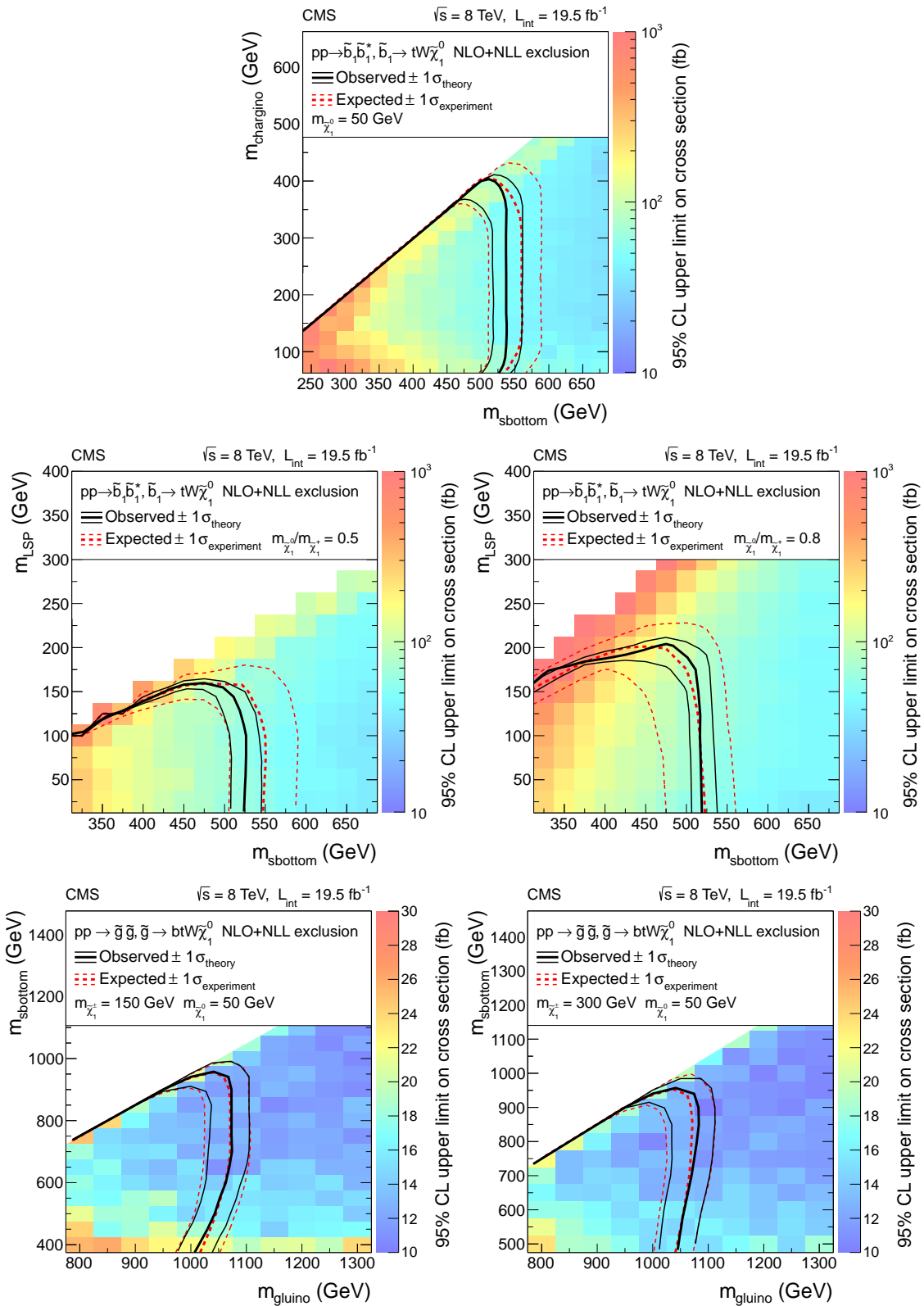


Figure 6: Exclusion regions at 95% CL in the planes of (top and center) $m(\tilde{\chi}_1^\pm)$ versus $m(\tilde{b}_1)$ and $m(\tilde{\chi}_1^0)$ versus $m(\tilde{b}_1)$ (model B1), and (bottom) $m(\tilde{b}_1)$ versus $m(\tilde{g})$ (model B2). The convention for the exclusion curves is the same as in Fig. 5.

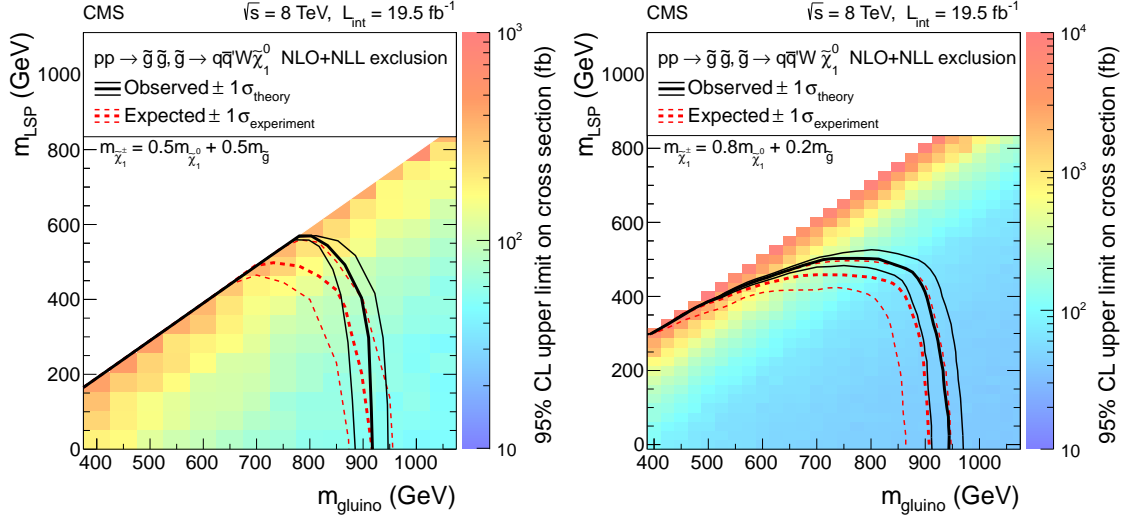


Figure 7: Exclusion regions at 95% CL in the planes of $m(\tilde{\chi}_1^0)$ versus $m(\tilde{g})$ for two different values of chargino mass (model C1). The convention for the exclusion curves is the same as in Fig. 5.

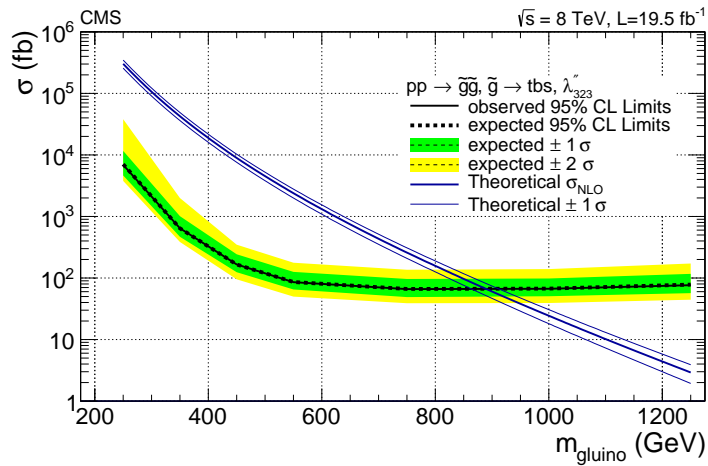


Figure 8: 95% CL upper limit on the gluino production cross section for an RPV simplified model, $pp \rightarrow \tilde{g}\tilde{g}, \tilde{g} \rightarrow t\bar{b}s$.

$m(\tilde{\chi}_1^0)$. A similar conclusion applies to model A2, since the final state is the same. For bottom-squark pair production, limits on $m(\tilde{b}_1)$ of about 600 GeV have been presented [46], but assuming the decay mode $\tilde{b}_1 \rightarrow b\tilde{\chi}_1^0$ instead of the model B1 mode $\tilde{b}_1 \rightarrow t\tilde{\chi}_1^-$ considered here. Comparable limits for model A1, as well as for similar models with top and bottom quarks from gluino decays, have been reported by the ATLAS Collaboration [48–51].

A single RPV scenario is considered in this analysis, one in which gluino pair production is followed by the decay of each gluino to three quarks, as is favoured in the SUSY model with minimal flavour violation [52]: $\tilde{g} \rightarrow fbs(\bar{f}\bar{b}\bar{s})$ (model RPV). Such decays lead to same-sign W-boson pairs in the final state in 50% of the cases. Compared with the decays $\tilde{g} \rightarrow tsd(\bar{t}\bar{s}\bar{d})$, which also yield same-sign W-boson pairs, the mode considered profits from having two extra b quarks in the final state, resulting in a higher signal selection efficiency. The model is governed by one parameter ($m_{\tilde{g}}$), which dictates the production cross section and the final state kinematics. The dedicated search region RPV2 with the high- p_T lepton selection is used to place an upper limit on the production cross section. The result is shown in Fig. 8. In this scenario, the gluino mass is probed up to approximately 900 GeV.

The results for the signal regions SStop1, SStop1++, SStop2, and SStop2++ are used to set limits on the cross section for same-sign top-quark pair production, $\sigma(\text{pp} \rightarrow \text{tt}, \bar{\text{t}}\bar{\text{t}})$ from SStop1 and SStop2, and $\sigma(\text{pp} \rightarrow \text{tt})$ from SStop1++ and SStop2++. Here $\sigma(\text{pp} \rightarrow \text{tt}, \bar{\text{t}}\bar{\text{t}})$ is shorthand for the sum $\sigma(\text{pp} \rightarrow \text{tt}) + \sigma(\text{pp} \rightarrow \bar{\text{t}}\bar{\text{t}})$. These limits are calculated using an acceptance obtained from simulated $\text{pp} \rightarrow \bar{\text{t}}\bar{\text{t}}$ events and an opposite-sign selection. This acceptance, including branching fractions, is 0.43% (0.26%) for the SStop1 (SStop2) search region. The relative uncertainty in this acceptance is 14%. The observed upper limits are $\sigma(\text{pp} \rightarrow \text{tt}, \bar{\text{t}}\bar{\text{t}}) < 720 \text{ fb}$ and $\sigma(\text{pp} \rightarrow \text{tt}) < 370 \text{ fb}$ at 95% CL. The median expected limits are $470_{-110}^{+180} \text{ fb}$ and $310_{-80}^{+110} \text{ fb}$, respectively.

Similarly, the results from signal regions SR21–SR28 with the high- p_T lepton selection are used to set limits on the SM cross section for quadruple top-quark production. The observed upper limit is $\sigma(\text{pp} \rightarrow \text{tt}\bar{\text{t}}\bar{\text{t}}) < 49 \text{ fb}$ at 95% CL, compared to a median expected limit of 36_{-9}^{+16} fb . The SM cross section as computed with the MC@NLO program [53] is $\sigma_{\text{SM}} = 0.914 \pm 0.005 \text{ fb}$. The most sensitive signal regions, SR24 and SR28, have a signal acceptance of 0.52% and 0.49%, respectively, with relative uncertainties of 13% and 17%.

9 Information for additional model testing

We have described a signature-based search that finds no evidence for physics beyond the SM. In Section 8, the results are used to place bounds on the parameters of a number of models of new physics. Here, additional information is presented that can be used to confront other models of new physics in an approximate way through MC generator-level studies. The expected numbers of events can then be compared with an upper limit on the number of signal events that can be obtained using inputs from Tables 7 and 8 and a signal acceptance uncertainty estimated from the generator-level studies.

The E_T^{miss} and H_T turn-on curves, shown in Fig. 9 as a function of the respective generator-level quantities, are parametrized as $0.5 \cdot \epsilon_\infty \cdot \{ \text{erf} [(x - x_{1/2})/\sigma] + 1 \}$, with $\text{erf}(z)$ the error function, and ϵ_∞ , $x_{1/2}$, and σ the parameters of the fit. The generator H_T is calculated using generator jets, obtained by clustering all stable particles from the hard collision, after showering and hadronization, except for neutrinos and other non-interacting particles. The parameters of the fitted functions are summarized in Tables 10 and 11 for E_T^{miss} and H_T , respectively. Analogously to the offline selection, only generator jets that are separated from generator electrons and muons by $\Delta R \equiv \sqrt{\Delta\phi^2 + \Delta\eta^2} > 0.4$ are considered in the derivation and application of the efficiency

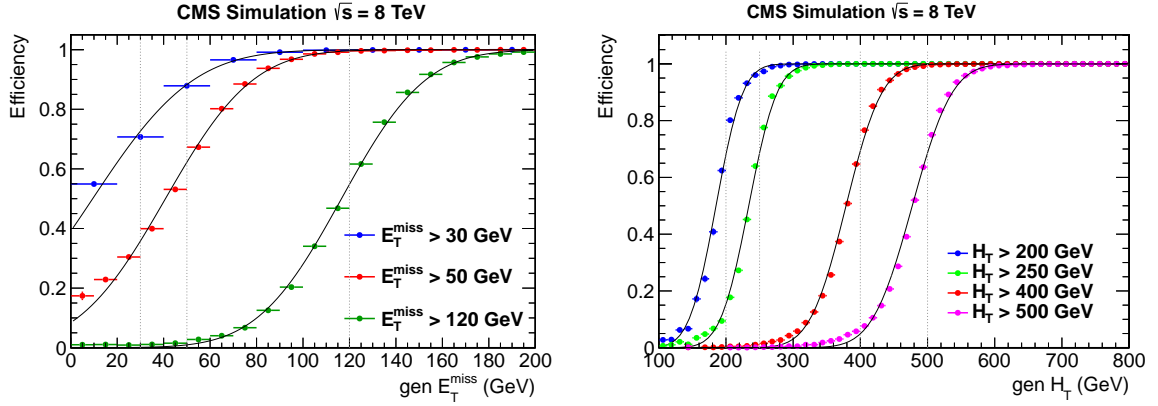


Figure 9: Efficiency for an event to satisfy a given reconstructed E_T^{miss} (H_T) threshold as a function of generator-level E_T^{miss} (H_T^{gen}). The curves are shown for E_T^{miss} thresholds of 30, 50, and 120 GeV; the thresholds for H_T are 200, 250, 400, and 500 GeV.

model. Only electrons and muons from the hard collision are considered. The separation between jets and leptons applies to the calculation of H_T as well as to the counting of jets and b-tagged jets. The generator-level E_T^{miss} is constructed as the vector sum p_T of all neutrinos, selected after showering and hadronization, and any other non-interacting particles from the hard collision.

Table 10: The resulting fit parameters for the efficiency curves presented in Fig. 9 left.

Parameter	$E_T^{\text{miss}} > 30$ GeV	$E_T^{\text{miss}} > 50$ GeV	$E_T^{\text{miss}} > 120$ GeV
ϵ_∞	1.000 ± 0.001	1.000 ± 0.001	0.999 ± 0.001
$x_{1/2}$ (GeV)	13.87 ± 0.30	42.97 ± 0.14	117.85 ± 0.09
σ (GeV)	42.92 ± 0.34	37.47 ± 0.20	36.90 ± 0.14

Table 11: The resulting fit parameters for the efficiency curves presented in Fig. 9 right.

Parameter	$H_T > 200$ GeV	$H_T > 250$ GeV	$H_T > 400$ GeV	$H_T > 500$ GeV
ϵ_∞	0.999 ± 0.001	0.999 ± 0.001	0.999 ± 0.001	0.999 ± 0.001
$x_{1/2}$ (GeV)	185.2 ± 0.4	233.9 ± 0.3	378.69 ± 0.17	477.3 ± 0.2
σ (GeV)	44.5 ± 0.6	46.9 ± 0.4	59.41 ± 0.26	66.05 ± 0.25

An additional turn-on curve, introduced since the publication of Ref. [11], has been added to parametrize the efficiency to reconstruct a jet with $p_T > 40$ GeV. The curve, shown in Fig. 10 (left) as a function of the generator jet p_T , is described by the same functional form as the H_T turn-on. The parameters of the fit are $(\epsilon_\infty, x_{1/2}, \sigma) = (1.0, 29.8 \text{ GeV}, 18.8 \text{ GeV})$.

Figure 10 also shows the b-tagging efficiency, obtained from simulation, for b quarks with $|\eta| < 2.4$. The efficiency is fit with a third-order (first-order) polynomial for $p_T < 120$ GeV ($p_T > 120$ GeV). The parameters of the fit are given in Table 12.

The turn-on curves for the lepton selection are shown in Fig. 11. The lepton efficiency (ϵ)—including the effects of reconstruction, identification, and isolation as well as relevant data-to-simulation scale factors—is parametrized as $\epsilon(p_T) = \epsilon_\infty \cdot \text{erf}[(p_T - 10)/\sigma] + \epsilon_{10} \cdot \{1 - \text{erf}[(p_T - 10)/\sigma]\}$. The results of the fit are summarized in Table 13.

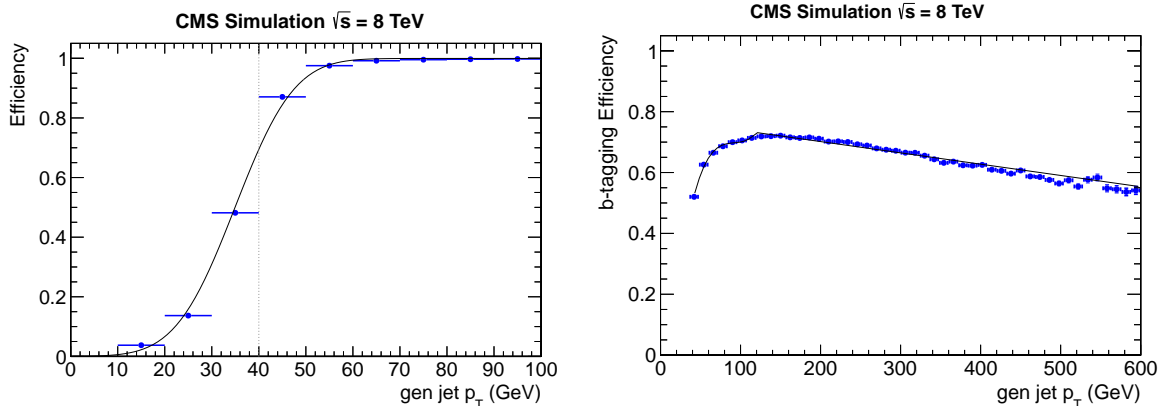


Figure 10: Efficiency for the reconstruction of jets with $p_T > 40$ GeV as a function of the generator jet p_T (left); b-tagging efficiency as a function of the p_T of the generator jet matched to a bottom quark from the hard collision (right).

Table 12: b-tagging efficiency parameters. A polynomial of form $Ax^3 + Bx^2 + Cx + D$ is used for $p_T < 120$ GeV while a linear fit, $Ex + F$, is performed above that threshold. Note that the parametrization is valid only for moderate range (i.e. [30–600] GeV) of b-quark jet p_T .

Parameter	Value
A	$(1.55 \pm 0.05) \times 10^{-6}$
B	$(-4.26 \pm 0.12) \times 10^{-4}$
C	0.0391 ± 0.0008
D	-0.496 ± 0.020
E	$(-3.26 \pm 0.01) \times 10^{-4}$
F	0.7681 ± 0.0016

Table 13: The parameters of the fit performed in Fig. 11 for electron and muon selection efficiencies.

Parameter	Electrons	Muons
ϵ_∞	0.640 ± 0.001	0.673 ± 0.001
ϵ_{10}	0.170 ± 0.002	0.332 ± 0.003
σ (GeV)	36.94 ± 0.320	29.65 ± 0.382

The prescription to apply the efficiency model is similar to that described in Ref. [14], with some modifications needed to accommodate the use of exclusive signal regions. The efficiencies for the H_T and E_T^{miss} selections in regions with upper and lower bounds are obtained by taking the difference between the relevant curves in Fig. 9. The jet reconstruction and b-tagging efficiencies are provided as per-jet quantities. Thus, one scale factor per jet should be obtained from the relevant curves. Additional combinatorial factors should be included, as dictated by the requirements of the signal region selection. The application of the lepton efficiency remains unchanged, with one factor per lepton obtained from the appropriate fit of Fig. 11. All the quoted efficiencies are multiplicative. The resulting signal yield, obtained by summing the contribution derived from the efficiency model over all events, is then compared to the calculated upper limit as described at the beginning of this section.

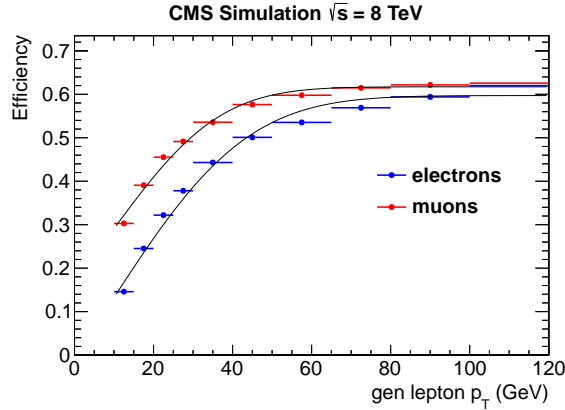


Figure 11: Electron and muon selection efficiency as a function of the generated lepton p_T .

The efficiency model presented was applied to a variety of the signal models and search regions considered in this analysis. Results from the efficiency model were found to agree with those obtained using the detector simulation and reconstruction to within approximately 30%. It should be emphasized that the efficiency model is approximate and is not universally applicable. Lepton isolation efficiency, for example, depends on the hadronic activity in the event and in some extreme cases on the event topology. For instance, in models giving rise to top quarks with a significant boost, the lepton isolation efficiency in Fig. 11 overestimates the true value.

10 Summary

We have presented the results of a search for physics beyond the standard model with same-sign dilepton events using the CMS detector at the LHC. The study is based on a sample of pp collisions at $\sqrt{s} = 8$ TeV corresponding to an integrated luminosity of 19.5 fb^{-1} . The data are analyzed in exclusive signal regions formed by placing different requirements on the discriminating variables H_T , E_T^{miss} , number of jets, and number of b-tagged jets. The latter can assume values of 0, 1, and 2 or more, which allow us to probe signatures both with and without third-generation squarks. No significant deviation from standard model expectation is observed.

Using sparticle production cross sections calculated in the decoupling limit, and assuming that gluinos decay exclusively into top or bottom squarks and that the top and bottom squarks decay as $\tilde{t}_1 \rightarrow t\tilde{\chi}_1^0$ and $\tilde{b}_1 \rightarrow t\tilde{\chi}_1^-$ ($\tilde{\chi}_1^- \rightarrow W^-\tilde{\chi}_1^0$), lower limits on gluino and sbottom masses are calculated. Gluinos with masses up to approximately 1050 GeV and bottom squarks with masses up to about 500 GeV are probed. In models where gluinos do not decay to third-generation squarks, sensitivity for gluino masses up to approximately 900 GeV is obtained. A similar reach in the gluino masses is demonstrated in the scope of an R -parity violating model.

The results are used to set upper limits on the same-sign top-quark pair production cross section $\sigma(\text{pp} \rightarrow \text{tt}, \bar{\text{t}}\bar{\text{t}}) < 720 \text{ fb}$ and $\sigma(\text{pp} \rightarrow \text{tt}) < 370 \text{ fb}$ at 95% CL. An upper limit at 95% CL of $\sigma(\text{pp} \rightarrow \text{tt}\bar{\text{t}}) < 49 \text{ fb}$ is obtained for the cross section of quadruple top-quark production.

Acknowledgements

We wish to congratulate our colleagues in the CERN accelerator departments for the excellent performance of the LHC machine. We thank the technical and administrative staff at CERN and

other CMS institutes, and acknowledge support from: FMSR (Austria); FNRS and FWO (Belgium); CNPq, CAPES, FAPERJ, and FAPESP (Brazil); MES (Bulgaria); CERN; CAS, MoST, and NSFC (China); COLCIENCIAS (Colombia); MSES (Croatia); RPF (Cyprus); Academy of Sciences and NICPB (Estonia); Academy of Finland, MEC, and HIP (Finland); CEA and CNRS/IN2P3 (France); BMBF, DFG, and HGF (Germany); GSRT (Greece); OTKA and NKTH (Hungary); DAE and DST (India); IPM (Iran); SFI (Ireland); INFN (Italy); NRF and WCU (Korea); LAS (Lithuania); CINVESTAV, CONACYT, SEP, and UASLP-FAI (Mexico); MSI (New Zealand); PAEC (Pakistan); MSHE and NSC (Poland); FCT (Portugal); JINR (Armenia, Belarus, Georgia, Ukraine, Uzbekistan); MON, RosAtom, RAS and RFBR (Russia); MSTD (Serbia); MICINN and CPAN (Spain); Swiss Funding Agencies (Switzerland); NSC (Taipei); TUBITAK and TAEK (Turkey); STFC (United Kingdom); DOE and NSF (USA).

Individuals have received support from the Marie-Curie programme and the European Research Council and EPLANET (European Union); the Leventis Foundation; the A. P. Sloan Foundation; the Alexander von Humboldt Foundation; the Belgian Federal Science Policy Office; the Fonds pour la Formation à la Recherche dans l'Industrie et dans l'Agriculture (FRIA-Belgium); the Agentschap voor Innovatie door Wetenschap en Technologie (IWT-Belgium); the Ministry of Education, Youth and Sports (MEYS) of Czech Republic; the Council of Science and Industrial Research, India; the Compagnia di San Paolo (Torino); the HOMING PLUS programme of Foundation for Polish Science, cofinanced by EU, Regional Development Fund; and the Thalys and Aristeia programmes cofinanced by EU-ESF and the Greek NSRF.

References

- [1] R. M. Barnett, J. F. Gunion, and H. E. Haber, "Discovering supersymmetry with like-sign dileptons", *Phys. Lett. B* **315** (1993) 349, doi:10.1016/0370-2693(93)91623-U, arXiv:hep-ph/9306204.
- [2] M. Guchait and D. P. Roy, "Like-sign dilepton signature for gluino production at CERN LHC including top quark and Higgs boson effects", *Phys. Rev. D* **52** (1995) 133, doi:10.1103/PhysRevD.52.133, arXiv:hep-ph/9412329.
- [3] H. Baer, C.-h. Chen, F. Paige, and X. Tata, "Signals for minimal supergravity at the CERN Large Hadron Collider. II. Multilepton channels", *Phys. Rev. D* **53** (1996) 6241, doi:10.1103/PhysRevD.53.6241, arXiv:hep-ph/9512383.
- [4] H.-C. Cheng, K. T. Matchev, and M. Schmaltz, "Bosonic supersymmetry? Getting fooled at the CERN LHC", *Phys. Rev. D* **66** (2002) 056006, doi:10.1103/PhysRevD.66.056006, arXiv:hep-ph/0205314.
- [5] R. Contino and G. Servant, "Discovering the top partners at the LHC using same-sign dilepton final states", *JHEP* **06** (2008) 026, doi:10.1088/1126-6708/2008/06/026, arXiv:0801.1679.
- [6] F. M. L. Almeida Jr. et al., "Same-sign dileptons as a signature for heavy Majorana neutrinos in hadron-hadron collisions", *Phys. Lett. B* **400** (1997) 331, doi:10.1016/S0370-2693(97)00143-3, arXiv:hep-ph/9703441.
- [7] Y. Bai and Z. Han, "Top-antitop and top-top resonances in the dilepton channel at the CERN LHC", *JHEP* **04** (2009) 056, doi:10.1088/1126-6708/2009/04/056, arXiv:0809.4487.

- [8] E. L. Berger et al., “Top Quark Forward-Backward Asymmetry and Same-Sign Top Quark Pairs”, *Phys. Rev. Lett.* **106** (2011) 201801, doi:10.1103/PhysRevLett.106.201801, arXiv:1101.5625.
- [9] J. L. Feng, “Dark Matter Candidates from Particle Physics and Methods of Detection”, *Ann. Rev. Astron. Astrophys.* **48** (2010) 495, doi:10.1146/annurev-astro-082708-101659, arXiv:1003.0904.
- [10] S. P. Martin, “A Supersymmetry Primer”, (1997). arXiv:hep-ph/9709356.
- [11] CMS Collaboration, “Search for new physics in events with same-sign dileptons and b jets in pp collisions at $\sqrt{s} = 8$ TeV”, *JHEP* **03** (2013) 037, doi:10.1007/JHEP03(2013)037, arXiv:1212.6194.
- [12] CMS Collaboration, “Search for new physics with same-sign isolated dilepton events with jets and missing transverse energy at the LHC”, *JHEP* **06** (2011) 077, doi:10.1007/JHEP06(2011)077, arXiv:1104.3168.
- [13] CMS Collaboration, “Search for new physics with same-sign isolated dilepton events with jets and missing transverse energy”, *Phys. Rev. Lett.* **109** (2012) 071803, doi:10.1103/PhysRevLett.109.071803, arXiv:1205.6615.
- [14] CMS Collaboration, “Search for new physics in events with same-sign dileptons and b-tagged jets in pp collisions at $\sqrt{s} = 7$ TeV”, *JHEP* **08** (2012) 110, doi:10.1007/JHEP08(2012)110, arXiv:1205.3933.
- [15] CMS Collaboration, “The CMS experiment at the CERN LHC”, *JINST* **3** (2008) S08004, doi:10.1088/1748-0221/3/08/S08004.
- [16] CMS Collaboration, “Identification of b-quark jets with the CMS experiment”, *JINST* **8** (2013) P04013, doi:10.1088/1748-0221/8/04/P04013, arXiv:1211.4462.
- [17] M. Cacciari and G. P. Salam, “Pileup subtraction using jet areas”, *Phys. Lett. B* **659** (2008) 119, doi:10.1016/j.physletb.2007.09.077, arXiv:0707.1378.
- [18] J. Alwall et al., “MADGRAPH 5: Going Beyond”, *JHEP* **06** (2011) 128, doi:10.1007/JHEP06(2011)128, arXiv:1106.0522.
- [19] GEANT4 Collaboration, “Geant4—a simulation toolkit”, *Nucl. Instrum. Meth. A* **506** (2003) 250, doi:10.1016/S0168-9002(03)01368-8.
- [20] P. M. Nadolsky et al., “Implications of CTEQ global analysis for collider observables”, *Phys. Rev. D* **78** (2008) 013004, doi:10.1103/PhysRevD.78.013004, arXiv:0802.0007.
- [21] T. Sjöstrand, S. Mrenna, and P. Z. Skands, “PYTHIA 6.4 physics and manual”, *JHEP* **05** (2006) 026, doi:10.1088/1126-6708/2006/05/026, arXiv:hep-ph/0603175.
- [22] S. Abdullin et al., “The fast simulation of the CMS detector at LHC”, *J. Phys. Conf. Ser.* **331** (2011) 032049, doi:10.1088/1742-6596/331/3/032049.
- [23] J. M. Campbell and R. K. Ellis, “ $t\bar{t}W^\pm$ production and decay at NLO”, *JHEP* **07** (2012) 052, doi:10.1007/JHEP07(2012)052, arXiv:1204.5678.

- [24] A. Kardos, Z. Trocsanyi, and C. Papadopoulos, "Top quark pair production in association with a Z-boson at next-to-leading-order accuracy", *Phys. Rev. D* **85** (2012) 054015, doi:10.1103/PhysRevD.85.054015, arXiv:1111.0610.
- [25] M. V. Garzelli, A. Kardos, C. G. Papadopoulos, and Z. Trocsanyi, " Z^0 -boson production in association with a $t\bar{t}$ pair at next-to-leading-order accuracy with parton shower effects", *Phys. Rev. D* **85** (2012) 074022, doi:10.1103/PhysRevD.85.074022, arXiv:1111.1444.
- [26] CMS Collaboration, "Determination of jet energy calibration and transverse momentum resolution in CMS", *JINST* **6** (2011) P11002, doi:10.1088/1748-0221/6/11/P11002, arXiv:1107.4277.
- [27] CMS Collaboration, "Search for top-squark pair production in the single-lepton final state in pp collisions at $\sqrt{s} = 8$ TeV", *EPJC* **73** (2013) 2677, doi:10.1140/epjc/s10052-013-2677-2, arXiv:1308.1586.
- [28] CMS Collaboration, "CMS Luminosity Based on Pixel Cluster Counting - Summer 2013 Update", CMS Physics Analysis Summary CMS-PAS-LUM-13-001, (2013).
- [29] Particle Data Group, "Review of Particle Physics (RPP)", *Phys. Rev. D* **86** (2012) 010001, doi:10.1103/PhysRevD.86.010001.
- [30] A. L. Read, "Presentation of search results: The CL_s technique", *J. Phys. G* **28** (2002) 2693, doi:10.1088/0954-3899/28/10/313.
- [31] T. Junk, "Confidence level computation for combining searches with small statistics", *Nucl. Instrum. Meth. A* **434** (1999) 435, doi:10.1016/S0168-9002(99)00498-2, arXiv:hep-ex/9902006.
- [32] ATLAS and CMS Collaborations, "Procedure for the LHC Higgs boson search combination in summer 2011", ATL-PHYS-PUB-2011-011, CMS NOTE-2011/005, (2011).
- [33] LHC New Physics Working Group, "Simplified models for LHC new physics searches", *J. Phys. G* **39** (2012) 105005, doi:10.1088/0954-3899/39/10/105005, arXiv:1105.2838.
- [34] W. Beenakker, R. Höpker, M. Spira, and P. M. Zerwas, "Squark and gluino production at hadron colliders", *Nucl. Phys. B* **492** (1997) 51, doi:10.1016/S0550-3213(97)80027-2, arXiv:hep-ph/9610490.
- [35] A. Kulesza and L. Motyka, "Threshold resummation for squark-antisquark and gluino-pair production at the LHC", *Phys. Rev. Lett.* **102** (2009) 111802, doi:10.1103/PhysRevLett.102.111802, arXiv:0807.2405.
- [36] A. Kulesza and L. Motyka, "Soft gluon resummation for the production of gluino-gluino and squark-antisquark pairs at the LHC", *Phys. Rev. D* **80** (2009) 095004, doi:10.1103/PhysRevD.80.095004, arXiv:0905.4749.
- [37] W. Beenakker et al., "Soft-gluon resummation for squark and gluino hadroproduction", *JHEP* **12** (2009) 041, doi:10.1088/1126-6708/2009/12/041, arXiv:0909.4418.
- [38] W. Beenakker et al., "Squark and gluino hadroproduction", *Int. J. Mod. Phys. A* **26** (2011) 2637, doi:10.1142/S0217751X11053560, arXiv:1105.1110.

- [39] M. Krämer et al., “Supersymmetry production cross sections in pp collisions at $\sqrt{s} = 7$ TeV”, (2012). arXiv:1206.2892.
- [40] B. S. Acharya et al., “Identifying Multi-Top Events from Gluino Decay at the LHC”, (2009). arXiv:0901.3367.
- [41] G. L. Kane, E. Kuflik, R. Lu, and L.-T. Wang, “Top channel for early SUSY discovery at the LHC”, *Phys. Rev. D* **84** (2011) 095004, doi:10.1103/PhysRevD.84.095004, arXiv:1101.1963.
- [42] R. Essig, E. Izaguirre, J. Kaplan, and J. G. Wacker, “Heavy flavor simplified models at the LHC”, *JHEP* **01** (2012) 074, doi:10.1007/JHEP01(2012)074, arXiv:1110.6443.
- [43] M. Papucci, J. T. Ruderman, and A. Weiler, “Natural SUSY endures”, *JHEP* **09** (2012) 035, doi:10.1007/JHEP09(2012)035, arXiv:1110.6926.
- [44] CMS Collaboration, “Interpretation of searches for supersymmetry with simplified models”, (2013). arXiv:1301.2175. Submitted to *Phys. Rev. D*.
- [45] CMS Collaboration, “Search for supersymmetry in final states with missing transverse energy and 0, 1, 2, or at least 3 b-quark jets in 7 TeV pp collisions using the variable α_T ”, *JHEP* **01** (2013) 077, doi:10.1007/JHEP01(2013)077, arXiv:1210.8115.
- [46] CMS Collaboration, “Search for supersymmetry in hadronic final states with missing transverse energy using the variables α_T and b-quark multiplicity in pp collisions at $\sqrt{s} = 8$ TeV”, *Eur. Phys. J. C* **73** (2013) 2568, doi:10.1140/epjc/s10052-013-2568-6, arXiv:1303.2985.
- [47] CMS Collaboration, “Search for gluino mediated bottom- and top-squark production in multijet final states in pp collisions at 8 TeV”, *Phys. Lett. B* **725** (2013) 243, doi:10.1016/j.physletb.2013.06.058, arXiv:1305.2390.
- [48] ATLAS Collaboration, “Search for Gluinos in Events with Two Same-Sign Leptons, Jets and Missing Transverse Momentum with the ATLAS Detector in pp Collisions at $\sqrt{s} = 7$ TeV”, *Phys. Rev. Lett.* **108** (2012) 241802, doi:10.1103/PhysRevLett.108.241802, arXiv:1203.5763.
- [49] ATLAS Collaboration, “Search for supersymmetry in pp collisions at $\sqrt{s} = 7$ TeV in final states with missing transverse momentum and b-jets with the ATLAS detector”, *Phys. Rev. D* **85** (2012) 112006, doi:10.1103/PhysRevD.85.112006, arXiv:1203.6193.
- [50] ATLAS Collaboration, “Search for top and bottom squarks from gluino pair production in final states with missing transverse energy and at least three b-jets with the ATLAS detector”, *Eur. Phys. J. C* **72** (2012) 2174, doi:10.1140/epjc/s10052-012-2174-z, arXiv:1207.4686.
- [51] ATLAS Collaboration, “Multi-channel search for squarks and gluinos in $\sqrt{s} = 7$ TeV pp collisions with the ATLAS detector”, *Eur. Phys. J. C* **73** (2013) 2362, doi:10.1140/epjc/s10052-013-2362-5, arXiv:1212.6149.
- [52] C. Csaki, Y. Grossman, and B. Heidenreich, “Minimal flavor violation SUSY: A Natural Theory for R-Parity Violation”, *Phys. Rev. D* **85** (2012) 095009, doi:10.1103/PhysRevD.85.095009, arXiv:1111.1239.

-
- [53] S. Frixione and B. R. Webber, “Matching NLO QCD computations and parton shower simulations”, *JHEP* **06** (2002) 029, doi:[10.1088/1126-6708/2002/06/029](https://doi.org/10.1088/1126-6708/2002/06/029), arXiv:[hep-ph/0204244](https://arxiv.org/abs/hep-ph/0204244).

A The CMS Collaboration

Yerevan Physics Institute, Yerevan, Armenia

S. Chatrchyan, V. Khachatryan, A.M. Sirunyan, A. Tumasyan

Institut für Hochenergiephysik der OeAW, Wien, Austria

W. Adam, T. Bergauer, M. Dragicevic, J. Erö, C. Fabjan¹, M. Friedl, R. Frühwirth¹, V.M. Ghete, C. Hartl, N. Hörmann, J. Hrubec, M. Jeitler¹, W. Kiesenhofer, V. Knünz, M. Krammer¹, I. Krätschmer, D. Liko, I. Mikulec, D. Rabady², B. Rahbaran, H. Rohringer, R. Schöfbeck, J. Strauss, A. Taurok, W. Treberer-Treberspurg, W. Waltenberger, C.-E. Wulz¹

National Centre for Particle and High Energy Physics, Minsk, Belarus

V. Mossolov, N. Shumeiko, J. Suarez Gonzalez

Universiteit Antwerpen, Antwerpen, Belgium

S. Alderweireldt, M. Bansal, S. Bansal, T. Cornelis, E.A. De Wolf, X. Janssen, A. Knutsson, S. Luyckx, L. Mucibello, S. Ochesanu, B. Roland, R. Rougny, H. Van Haeevermaet, P. Van Mechelen, N. Van Remortel, A. Van Spilbeeck

Vrije Universiteit Brussel, Brussel, Belgium

F. Blekman, S. Blyweert, J. D'Hondt, N. Heracleous, A. Kalogeropoulos, J. Keaveney, T.J. Kim, S. Lowette, M. Maes, A. Olbrechts, D. Strom, S. Tavernier, W. Van Doninck, P. Van Mulders, G.P. Van Onsem, I. Villella

Université Libre de Bruxelles, Bruxelles, Belgium

C. Caillol, B. Clerboux, G. De Lentdecker, L. Favart, A.P.R. Gay, T. Hreus, A. Léonard, P.E. Marage, A. Mohammadi, L. Perniè, T. Reis, T. Seva, L. Thomas, C. Vander Velde, P. Vanlaer, J. Wang

Ghent University, Ghent, Belgium

V. Adler, K. Beernaert, L. Benucci, A. Cimmino, S. Costantini, S. Dildick, G. Garcia, B. Klein, J. Lellouch, J. McCartin, A.A. Ocampo Rios, D. Ryckbosch, M. Sigamani, N. Strobbe, F. Thyssen, M. Tytgat, S. Walsh, E. Yazgan, N. Zaganidis

Université Catholique de Louvain, Louvain-la-Neuve, Belgium

S. Basegmez, C. Beluffi³, G. Bruno, R. Castello, A. Caudron, L. Ceard, G.G. Da Silveira, C. Delaere, T. du Pree, D. Favart, L. Forthomme, A. Giammanco⁴, J. Hollar, P. Jez, M. Komm, V. Lemaître, J. Liao, O. Militaru, C. Nuttens, D. Pagano, A. Pin, K. Piotrkowski, A. Popov⁵, L. Quertenmont, M. Selvaggi, M. Vidal Marono, J.M. Vizan Garcia

Université de Mons, Mons, Belgium

N. Bely, T. Caebergs, E. Daubie, G.H. Hammad

Centro Brasileiro de Pesquisas Físicas, Rio de Janeiro, Brazil

G.A. Alves, M. Correa Martins Junior, T. Martins, M.E. Pol, M.H.G. Souza

Universidade do Estado do Rio de Janeiro, Rio de Janeiro, Brazil

W.L. Aldá Júnior, W. Carvalho, J. Chinellato⁶, A. Custódio, E.M. Da Costa, D. De Jesus Damiao, C. De Oliveira Martins, S. Fonseca De Souza, H. Malbouisson, M. Malek, D. Matos Figueiredo, L. Mundim, H. Nogima, W.L. Prado Da Silva, J. Santaolalla, A. Santoro, A. Sznajder, E.J. Tonelli Manganote⁶, A. Vilela Pereira

Universidade Estadual Paulista ^a, Universidade Federal do ABC ^b, São Paulo, Brazil

C.A. Bernardes^b, F.A. Dias^{a,7}, T.R. Fernandez Perez Tomei^a, E.M. Gregores^b, C. Lagana^a, P.G. Mercadante^b, S.F. Novaes^a, Sandra S. Padula^a

Institute for Nuclear Research and Nuclear Energy, Sofia, Bulgaria

V. Genchev², P. Iaydjiev², A. Marinov, S. Piperov, M. Rodozov, G. Sultanov, M. Vutova

University of Sofia, Sofia, Bulgaria

A. Dimitrov, I. Glushkov, R. Hadjiiska, V. Kozhuharov, L. Litov, B. Pavlov, P. Petkov

Institute of High Energy Physics, Beijing, China

J.G. Bian, G.M. Chen, H.S. Chen, M. Chen, R. Du, C.H. Jiang, D. Liang, S. Liang, X. Meng, R. Plestina⁸, J. Tao, X. Wang, Z. Wang

State Key Laboratory of Nuclear Physics and Technology, Peking University, Beijing, China

C. Asawatrangkuldee, Y. Ban, Y. Guo, Q. Li, W. Li, S. Liu, Y. Mao, S.J. Qian, D. Wang, L. Zhang, W. Zou

Universidad de Los Andes, Bogota, Colombia

C. Avila, C.A. Carrillo Montoya, L.F. Chaparro Sierra, C. Florez, J.P. Gomez, B. Gomez Moreno, J.C. Sanabria

Technical University of Split, Split, Croatia

N. Godinovic, D. Lelas, D. Polic, I. Puljak

University of Split, Split, Croatia

Z. Antunovic, M. Kovac

Institute Rudjer Boskovic, Zagreb, Croatia

V. Brigljevic, K. Kadija, J. Luetic, D. Mekterovic, S. Morovic, L. Tikvica

University of Cyprus, Nicosia, Cyprus

A. Attikis, G. Mavromanolakis, J. Mousa, C. Nicolaou, F. Ptochos, P.A. Razis

Charles University, Prague, Czech Republic

M. Finger, M. Finger Jr.

Academy of Scientific Research and Technology of the Arab Republic of Egypt, Egyptian Network of High Energy Physics, Cairo, Egypt

A.A. Abdelalim⁹, Y. Assran¹⁰, S. Elgammal⁹, A. Ellithi Kamel¹¹, M.A. Mahmoud¹², A. Radi^{13,14}

National Institute of Chemical Physics and Biophysics, Tallinn, Estonia

M. Kadastik, M. Müntel, M. Murumaa, M. Raidal, L. Rebane, A. Tiko

Department of Physics, University of Helsinki, Helsinki, Finland

P. Eerola, G. Fedi, M. Voutilainen

Helsinki Institute of Physics, Helsinki, Finland

J. Härkönen, V. Karimäki, R. Kinnunen, M.J. Kortelainen, T. Lampén, K. Lassila-Perini, S. Lehti, T. Lindén, P. Luukka, T. Mäenpää, T. Peltola, E. Tuominen, J. Tuominiemi, E. Tuovinen, L. Wendland

Lappeenranta University of Technology, Lappeenranta, Finland

T. Tuuva

DSM/IRFU, CEA/Saclay, Gif-sur-Yvette, France

M. Besancon, F. Couderc, M. Dejardin, D. Denegri, B. Fabbro, J.L. Faure, F. Ferri, S. Ganjour, A. Givernaud, P. Gras, G. Hamel de Monchenault, P. Jarry, E. Locci, J. Malcles, A. Nayak, J. Rander, A. Rosowsky, M. Titov

Laboratoire Leprince-Ringuet, Ecole Polytechnique, IN2P3-CNRS, Palaiseau, France

S. Baffioni, F. Beaudette, P. Busson, C. Charlot, N. Daci, T. Dahms, M. Dalchenko, L. Dobrzynski, A. Florent, R. Granier de Cassagnac, M. Haguenaer, P. Miné, C. Mironov, I.N. Naranjo, M. Nguyen, C. Ochando, P. Paganini, D. Sabes, R. Salerno, Y. Sirois, C. Veelken, Y. Yilmaz, A. Zabi

Institut Pluridisciplinaire Hubert Curien, Université de Strasbourg, Université de Haute Alsace Mulhouse, CNRS/IN2P3, Strasbourg, France

J.-L. Agram¹⁵, J. Andrea, D. Bloch, J.-M. Brom, E.C. Chabert, C. Collard, E. Conte¹⁵, F. Drouhin¹⁵, J.-C. Fontaine¹⁵, D. Gelé, U. Goerlach, C. Goetzmann, P. Juillot, A.-C. Le Bihan, P. Van Hove

Centre de Calcul de l'Institut National de Physique Nucleaire et de Physique des Particules, CNRS/IN2P3, Villeurbanne, France

S. Gadrat

Université de Lyon, Université Claude Bernard Lyon 1, CNRS-IN2P3, Institut de Physique Nucléaire de Lyon, Villeurbanne, France

S. Beauceron, N. Beaupere, G. Boudoul, S. Brochet, J. Chasserat, R. Chierici, D. Contardo, P. Depasse, H. El Mamouni, J. Fan, J. Fay, S. Gascon, M. Gouzevitch, B. Ille, T. Kurca, M. Lethuillier, L. Mirabito, S. Perries, J.D. Ruiz Alvarez¹⁶, L. Sgandurra, V. Sordini, M. Vander Donckt, P. Verdier, S. Viret, H. Xiao

E. Andronikashvili Institute of Physics, Academy of Science, Tbilisi, Georgia

L. Rurua

RWTH Aachen University, I. Physikalisches Institut, Aachen, Germany

C. Autermann, S. Beranek, M. Bontenackels, B. Calpas, M. Edelhoff, L. Feld, O. Hindrichs, K. Klein, A. Ostapchuk, A. Perieanu, F. Raupach, J. Sammet, S. Schael, D. Sprenger, H. Weber, B. Wittmer, V. Zhukov⁵

RWTH Aachen University, III. Physikalisches Institut A, Aachen, Germany

M. Ata, J. Caudron, E. Dietz-Laursonn, D. Duchardt, M. Erdmann, R. Fischer, A. Güth, T. Hebbeker, C. Heidemann, K. Hoepfner, D. Klingebiel, S. Knutzen, P. Kreuzer, M. Merschmeyer, A. Meyer, M. Olschewski, K. Padeken, P. Papacz, H. Pieta, H. Reithler, S.A. Schmitz, L. Sonnenschein, D. Teyssier, S. Thüer, M. Weber

RWTH Aachen University, III. Physikalisches Institut B, Aachen, Germany

V. Cherepanov, Y. Erdogan, G. Flügge, H. Geenen, M. Geisler, W. Haj Ahmad, F. Hoehle, B. Kargoll, T. Kress, Y. Kuessel, J. Lingemann², A. Nowack, I.M. Nugent, L. Perchalla, O. Pooth, A. Stahl

Deutsches Elektronen-Synchrotron, Hamburg, Germany

I. Asin, N. Bartosik, J. Behr, W. Behrenhoff, U. Behrens, A.J. Bell, M. Bergholz¹⁷, A. Bethani, K. Borras, A. Burgmeier, A. Cakir, L. Calligaris, A. Campbell, S. Choudhury, F. Costanza, C. Diez Pardos, S. Dooling, T. Dorland, G. Eckerlin, D. Eckstein, T. Eichhorn, G. Flucke, A. Geiser, A. Grebenyuk, P. Gunnellini, S. Habib, J. Hauk, G. Hellwig, M. Hempel, D. Horton, H. Jung, M. Kasemann, P. Katsas, C. Kleinwort, H. Kluge, M. Krämer, D. Krücker, W. Lange, J. Leonard, K. Lipka, W. Lohmann¹⁷, B. Lutz, R. Mankel, I. Marfin, I.-A. Melzer-Pellmann, A.B. Meyer, J. Mnich, A. Mussgiller, S. Naumann-Emme, O. Novgorodova, F. Nowak, J. Olzem, H. Perrey, A. Petrukhin, D. Pitzl, R. Placakyte, A. Raspereza, P.M. Ribeiro Cipriano, C. Riedl, E. Ron, M.Ö. Sahin, J. Salfeld-Nebgen, R. Schmidt¹⁷, T. Schoerner-Sadenius, M. Schröder, N. Sen, M. Stein, A.D.R. Vargas Trevino, R. Walsh, C. Wissing

University of Hamburg, Hamburg, Germany

M. Aldaya Martin, V. Blobel, H. Enderle, J. Erfle, E. Garutti, M. Görner, M. Gosselink, J. Haller, K. Heine, R.S. Höing, H. Kirschenmann, R. Klanner, R. Kogler, J. Lange, I. Marchesini, J. Ott, T. Peiffer, N. Pietsch, D. Rathjens, C. Sander, H. Schettler, P. Schleper, E. Schlieckau, A. Schmidt, T. Schum, M. Seidel, J. Sibille¹⁸, V. Sola, H. Stadie, G. Steinbrück, D. Troendle, E. Usai, L. Vanelderen

Institut für Experimentelle Kernphysik, Karlsruhe, Germany

C. Barth, C. Baus, J. Berger, C. Böser, E. Butz, T. Chwalek, W. De Boer, A. Descroix, A. Dierlamm, M. Feindt, M. Guthoff², F. Hartmann², T. Hauth², H. Held, K.H. Hoffmann, U. Husemann, I. Katkov⁵, A. Kornmayer², E. Kuznetsova, P. Lobelle Pardo, D. Martschei, M.U. Mozer, Th. Müller, M. Niegel, A. Nürnberg, O. Oberst, G. Quast, K. Rabbertz, F. Ratnikov, S. Röcker, F.-P. Schilling, G. Schott, H.J. Simonis, F.M. Stober, R. Ulrich, J. Wagner-Kuhr, S. Wayand, T. Weiler, R. Wolf, M. Zeise

Institute of Nuclear and Particle Physics (INPP), NCSR Demokritos, Aghia Paraskevi, Greece

G. Anagnostou, G. Daskalakis, T. Geralis, S. Kesisoglou, A. Kyriakis, D. Loukas, A. Markou, C. Markou, E. Ntomari, I. Topsis-giotis

University of Athens, Athens, Greece

L. Gouskos, A. Panagiotou, N. Saoulidou, E. Stiliaris

University of Ioánnina, Ioánnina, Greece

X. Aslanoglou, I. Evangelou, G. Flouris, C. Foudas, P. Kokkas, N. Manthos, I. Papadopoulos, E. Paradis

Wigner Research Centre for Physics, Budapest, Hungary

G. Bencze, C. Hajdu, P. Hidas, D. Horvath¹⁹, F. Sikler, V. Veszpremi, G. Vesztergombi²⁰, A.J. Zsigmond

Institute of Nuclear Research ATOMKI, Debrecen, Hungary

N. Beni, S. Czellar, J. Molnar, J. Palinkas, Z. Szillasi

University of Debrecen, Debrecen, Hungary

J. Karacsi, P. Raics, Z.L. Trocsanyi, B. Ujvari

National Institute of Science Education and Research, Bhubaneswar, India

S.K. Swain²¹

Panjab University, Chandigarh, India

S.B. Beri, V. Bhatnagar, N. Dhingra, R. Gupta, M. Kaur, M.Z. Mehta, M. Mittal, N. Nishu, A. Sharma, J.B. Singh

University of Delhi, Delhi, India

Ashok Kumar, Arun Kumar, S. Ahuja, A. Bhardwaj, B.C. Choudhary, A. Kumar, S. Malhotra, M. Naimuddin, K. Ranjan, P. Saxena, V. Sharma, R.K. Shivpuri

Saha Institute of Nuclear Physics, Kolkata, India

S. Banerjee, S. Bhattacharya, K. Chatterjee, S. Dutta, B. Gomber, Sa. Jain, Sh. Jain, R. Khurana, A. Modak, S. Mukherjee, D. Roy, S. Sarkar, M. Sharan, A.P. Singh

Bhabha Atomic Research Centre, Mumbai, India

A. Abdulsalam, D. Dutta, S. Kailas, V. Kumar, A.K. Mohanty², L.M. Pant, P. Shukla, A. Topkar

Tata Institute of Fundamental Research - EHEP, Mumbai, India

T. Aziz, R.M. Chatterjee, S. Ganguly, S. Ghosh, M. Guchait²², A. Gurtu²³, G. Kole, S. Kumar, M. Maity²⁴, G. Majumder, K. Mazumdar, G.B. Mohanty, B. Parida, K. Sudhakar, N. Wickramage²⁵

Tata Institute of Fundamental Research - HECR, Mumbai, India

S. Banerjee, S. Dugad

Institute for Research in Fundamental Sciences (IPM), Tehran, Iran

H. Arfaei, H. Bakhshiansohi, H. Behnamian, S.M. Etesami²⁶, A. Fahim²⁷, A. Jafari, M. Khakzad, M. Mohammadi Najafabadi, M. Naseri, S. Paktinat Mehdiabadi, B. Safarzadeh²⁸, M. Zeinali

University College Dublin, Dublin, Ireland

M. Grunewald

INFN Sezione di Bari ^a, Università di Bari ^b, Politecnico di Bari ^c, Bari, Italy

M. Abbrescia^{a,b}, L. Barbone^{a,b}, C. Calabria^{a,b}, S.S. Chhibra^{a,b}, A. Colaleo^a, D. Creanza^{a,c}, N. De Filippis^{a,c}, M. De Palma^{a,b}, L. Fiore^a, G. Iaselli^{a,c}, G. Maggi^{a,c}, M. Maggi^a, B. Marangelli^{a,b}, S. My^{a,c}, S. Nuzzo^{a,b}, N. Pacifico^a, A. Pompili^{a,b}, G. Pugliese^{a,c}, R. Radogna^{a,b}, G. Selvaggi^{a,b}, L. Silvestris^a, G. Singh^{a,b}, R. Venditti^{a,b}, P. Verwilligen^a, G. Zito^a

INFN Sezione di Bologna ^a, Università di Bologna ^b, Bologna, Italy

G. Abbiendi^a, A.C. Benvenuti^a, D. Bonacorsi^{a,b}, S. Braibant-Giacomelli^{a,b}, L. Brigliadori^{a,b}, R. Campanini^{a,b}, P. Capiluppi^{a,b}, A. Castro^{a,b}, F.R. Cavallo^a, G. Codispoti^{a,b}, M. Cuffiani^{a,b}, G.M. Dallavalle^a, F. Fabbri^a, A. Fanfani^{a,b}, D. Fasanella^{a,b}, P. Giacomelli^a, C. Grandi^a, L. Guiducci^{a,b}, S. Marcellini^a, G. Masetti^a, M. Meneghelli^{a,b}, A. Montanari^a, F.L. Navarria^{a,b}, F. Odorici^a, A. Perrotta^a, F. Primavera^{a,b}, A.M. Rossi^{a,b}, T. Rovelli^{a,b}, G.P. Siroli^{a,b}, N. Tosi^{a,b}, R. Travaglini^{a,b}

INFN Sezione di Catania ^a, Università di Catania ^b, CSFNSM ^c, Catania, Italy

S. Albergo^{a,b}, G. Cappello^a, M. Chiorboli^{a,b}, S. Costa^{a,b}, F. Giordano^{a,2}, R. Potenza^{a,b}, A. Tricomi^{a,b}, C. Tuve^{a,b}

INFN Sezione di Firenze ^a, Università di Firenze ^b, Firenze, Italy

G. Barbagli^a, V. Ciulli^{a,b}, C. Civinini^a, R. D'Alessandro^{a,b}, E. Focardi^{a,b}, E. Gallo^a, S. Gonzi^{a,b}, V. Gori^{a,b}, P. Lenzi^{a,b}, M. Meschini^a, S. Paoletti^a, G. Sguazzoni^a, A. Tropiano^{a,b}

INFN Laboratori Nazionali di Frascati, Frascati, Italy

L. Benussi, S. Bianco, F. Fabbri, D. Piccolo

INFN Sezione di Genova ^a, Università di Genova ^b, Genova, Italy

P. Fabbricatore^a, R. Ferretti^{a,b}, F. Ferro^a, M. Lo Vetere^{a,b}, R. Musenich^a, E. Robutti^a, S. Tosi^{a,b}

INFN Sezione di Milano-Bicocca ^a, Università di Milano-Bicocca ^b, Milano, Italy

A. Benaglia^a, M.E. Dinardo^{a,b}, S. Fiorendi^{a,b,2}, S. Gennai^a, A. Ghezzi^{a,b}, P. Govoni^{a,b}, M.T. Lucchini^{a,b,2}, S. Malvezzi^a, R.A. Manzoni^{a,b,2}, A. Martelli^{a,b,2}, D. Menasce^a, L. Moroni^a, M. Paganoni^{a,b}, D. Pedrini^a, S. Ragazzi^{a,b}, N. Redaelli^a, T. Tabarelli de Fatis^{a,b}

INFN Sezione di Napoli ^a, Università di Napoli 'Federico II' ^b, Università della Basilicata (Potenza) ^c, Università G. Marconi (Roma) ^d, Napoli, Italy

S. Buontempo^a, N. Cavallo^{a,c}, F. Fabozzi^{a,c}, A.O.M. Iorio^{a,b}, L. Lista^a, S. Meola^{a,d,2}, M. Merola^a, P. Paolucci^{a,2}

INFN Sezione di Padova ^a, Università di Padova ^b, Università di Trento (Trento) ^c, Padova, Italy

P. Azzi^a, N. Bacchetta^a, D. Bisello^{a,b}, A. Branca^{a,b}, R. Carlin^{a,b}, P. Checchia^a, T. Dorigo^a, U. Dosselli^a, M. Galanti^{a,b,2}, F. Gasparini^{a,b}, U. Gasparini^{a,b}, P. Giubilato^{a,b}, A. Gozzelino^a, K. Kanishchev^{a,c}, S. Lacaprara^a, I. Lazzizzera^{a,c}, M. Margoni^{a,b}, A.T. Meneguzzo^{a,b}, M. Passaseo^a, J. Pazzini^{a,b}, M. Pegoraro^a, N. Pozzobon^{a,b}, P. Ronchese^{a,b}, F. Simonetto^{a,b}, E. Torassa^a, M. Tosi^{a,b}, S. Vanini^{a,b}, P. Zotto^{a,b}, A. Zucchetta^{a,b}, G. Zumerle^{a,b}

INFN Sezione di Pavia ^a, Università di Pavia ^b, Pavia, Italy

M. Gabusi^{a,b}, S.P. Ratti^{a,b}, C. Riccardi^{a,b}, P. Vitulo^{a,b}

INFN Sezione di Perugia ^a, Università di Perugia ^b, Perugia, Italy

M. Biasini^{a,b}, G.M. Bilei^a, L. Fanò^{a,b}, P. Lariccia^{a,b}, G. Mantovani^{a,b}, M. Menichelli^a, A. Nappi^{a,b†}, F. Romeo^{a,b}, A. Saha^a, A. Santocchia^{a,b}, A. Spiezia^{a,b}

INFN Sezione di Pisa ^a, Università di Pisa ^b, Scuola Normale Superiore di Pisa ^c, Pisa, Italy

K. Androsov^{a,29}, P. Azzurri^a, G. Bagliesi^a, J. Bernardini^a, T. Boccali^a, G. Broccolo^{a,c}, R. Castaldi^a, M.A. Ciocci^{a,29}, R. Dell'Orso^a, F. Fiori^{a,c}, L. Foà^{a,c}, A. Giassi^a, M.T. Grippo^{a,29}, A. Kraan^a, F. Ligabue^{a,c}, T. Lomtadze^a, L. Martini^{a,b}, A. Messineo^{a,b}, C.S. Moon^{a,30}, F. Palla^a, A. Rizzi^{a,b}, A. Savoy-Navarro^{a,31}, A.T. Serban^a, P. Spagnolo^a, P. Squillacioti^{a,29}, R. Tenchini^a, G. Tonelli^{a,b}, A. Venturi^a, P.G. Verdini^a, C. Vernieri^{a,c}

INFN Sezione di Roma ^a, Università di Roma ^b, Roma, Italy

L. Barone^{a,b}, F. Cavallari^a, D. Del Re^{a,b}, M. Diemoz^a, M. Grassi^{a,b}, C. Jorda^a, E. Longo^{a,b}, F. Margaroli^{a,b}, P. Meridiani^a, F. Micheli^{a,b}, S. Nourbakhsh^{a,b}, G. Organtini^{a,b}, R. Paramatti^a, S. Rahatlou^{a,b}, C. Rovelli^a, L. Soffi^{a,b}, P. Traczyk^{a,b}

INFN Sezione di Torino ^a, Università di Torino ^b, Università del Piemonte Orientale (Novara) ^c, Torino, Italy

N. Amapane^{a,b}, R. Arcidiacono^{a,c}, S. Argiro^{a,b}, M. Arneodo^{a,c}, R. Bellan^{a,b}, C. Biino^a, N. Cartiglia^a, S. Casasso^{a,b}, M. Costa^{a,b}, A. Degano^{a,b}, N. Demaria^a, C. Mariotti^a, S. Maselli^a, E. Migliore^{a,b}, V. Monaco^{a,b}, M. Musich^a, M.M. Obertino^{a,c}, G. Ortona^{a,b}, L. Pacher^{a,b}, N. Pastrone^a, M. Pelliccioni^{a,2}, A. Potenza^{a,b}, A. Romero^{a,b}, M. Ruspa^{a,c}, R. Sacchi^{a,b}, A. Solano^{a,b}, A. Staiano^a, U. Tamponi^a

INFN Sezione di Trieste ^a, Università di Trieste ^b, Trieste, Italy

S. Belforte^a, V. Candelise^{a,b}, M. Casarsa^a, F. Cossutti^{a,2}, G. Della Ricca^{a,b}, B. Gobbo^a, C. La Licata^{a,b}, M. Marone^{a,b}, D. Montanino^{a,b}, A. Penzo^a, A. Schizzi^{a,b}, T. Umer^{a,b}, A. Zanetti^a

Kangwon National University, Chunchon, Korea

S. Chang, T.Y. Kim, S.K. Nam

Kyungpook National University, Daegu, Korea

D.H. Kim, G.N. Kim, J.E. Kim, D.J. Kong, S. Lee, Y.D. Oh, H. Park, D.C. Son

Chonnam National University, Institute for Universe and Elementary Particles, Kwangju, Korea

J.Y. Kim, Zero J. Kim, S. Song

Korea University, Seoul, Korea

S. Choi, D. Gyun, B. Hong, M. Jo, H. Kim, Y. Kim, K.S. Lee, S.K. Park, Y. Roh

University of Seoul, Seoul, Korea

M. Choi, J.H. Kim, C. Park, I.C. Park, S. Park, G. Ryu

Sungkyunkwan University, Suwon, Korea

Y. Choi, Y.K. Choi, J. Goh, M.S. Kim, E. Kwon, B. Lee, J. Lee, S. Lee, H. Seo, I. Yu

Vilnius University, Vilnius, Lithuania

I. Grigelionis, A. Juodagalvis

Centro de Investigacion y de Estudios Avanzados del IPN, Mexico City, Mexico

H. Castilla-Valdez, E. De La Cruz-Burelo, I. Heredia-de La Cruz³², R. Lopez-Fernandez, J. Martínez-Ortega, A. Sanchez-Hernandez, L.M. Villasenor-Cendejas

Universidad Iberoamericana, Mexico City, Mexico

S. Carrillo Moreno, F. Vazquez Valencia

Benemerita Universidad Autonoma de Puebla, Puebla, Mexico

H.A. Salazar Ibarguen

Universidad Autónoma de San Luis Potosí, San Luis Potosí, Mexico

E. Casimiro Linares, A. Morelos Pineda

University of Auckland, Auckland, New Zealand

D. Krofcheck

University of Canterbury, Christchurch, New Zealand

P.H. Butler, R. Doesburg, S. Reucroft, H. Silverwood

National Centre for Physics, Quaid-I-Azam University, Islamabad, Pakistan

M. Ahmad, M.I. Asghar, J. Butt, H.R. Hoorani, S. Khalid, W.A. Khan, T. Khurshid, S. Qazi, M.A. Shah, M. Shoaib

National Centre for Nuclear Research, Swierk, Poland

H. Bialkowska, M. Bluj³³, B. Boimska, T. Frueboes, M. Górski, M. Kazana, K. Nawrocki, K. Romanowska-Rybinska, M. Szleper, G. Wrochna, P. Zalewski

Institute of Experimental Physics, Faculty of Physics, University of Warsaw, Warsaw, Poland

G. Brona, K. Bunkowski, M. Cwiok, W. Dominik, K. Doroba, A. Kalinowski, M. Konecki, J. Krolikowski, M. Misiura, W. Wolszczak

Laboratório de Instrumentação e Física Experimental de Partículas, Lisboa, Portugal

P. Bargassa, C. Beirão Da Cruz E Silva, P. Faccioli, P.G. Ferreira Parracho, M. Gallinaro, F. Nguyen, J. Rodrigues Antunes, J. Seixas², J. Varela, P. Vischia

Joint Institute for Nuclear Research, Dubna, Russia

S. Afanasiev, I. Golutvin, I. Gorbunov, A. Kamenev, V. Karjavin, V. Konoplyanikov, G. Kozlov, A. Lanev, A. Malakhov, V. Matveev, P. Moisenz, V. Palichik, V. Perelygin, M. Savina, S. Shmatov, N. Skatchkov, V. Smirnov, A. Zarubin

Petersburg Nuclear Physics Institute, Gatchina (St. Petersburg), Russia

V. Golovtsov, Y. Ivanov, V. Kim, P. Levchenko, V. Murzin, V. Oreshkin, I. Smirnov, V. Sulimov, L. Uvarov, S. Vavilov, A. Vorobyev, An. Vorobyev

Institute for Nuclear Research, Moscow, Russia

Yu. Andreev, A. Dermenev, S. Gninenko, N. Golubev, M. Kirsanov, N. Krasnikov, A. Pashenkov, D. Tlisov, A. Toropin

Institute for Theoretical and Experimental Physics, Moscow, Russia

V. Epshteyn, V. Gavrilov, N. Lychkovskaya, V. Popov, G. Safronov, S. Semenov, A. Spiridonov, V. Stolin, E. Vlasov, A. Zhokin

P.N. Lebedev Physical Institute, Moscow, Russia

V. Andreev, M. Azarkin, I. Dremin, M. Kirakosyan, A. Leonidov, G. Mesyats, S.V. Rusakov, A. Vinogradov

Skobeltsyn Institute of Nuclear Physics, Lomonosov Moscow State University, Moscow, Russia

A. Belyaev, E. Boos, V. Bunichev, M. Dubinin⁷, L. Dudko, A. Ershov, A. Gribushin, V. Klyukhin, O. Kodolova, I. Lokhtin, A. Markina, S. Obraztsov, S. Petrushanko, V. Savrin

State Research Center of Russian Federation, Institute for High Energy Physics, Protvino, Russia

I. Azhgirey, I. Bayshev, S. Bitioukov, V. Kachanov, A. Kalinin, D. Konstantinov, V. Krychkin, V. Petrov, R. Ryutin, A. Sobol, L. Tourtchanovitch, S. Troshin, N. Tyurin, A. Uzunian, A. Volkov

University of Belgrade, Faculty of Physics and Vinca Institute of Nuclear Sciences, Belgrade, Serbia

P. Adzic³⁴, M. Djordjevic, M. Ekmedzic, J. Milosevic

Centro de Investigaciones Energéticas Medioambientales y Tecnológicas (CIEMAT), Madrid, Spain

M. Aguilar-Benitez, J. Alcaraz Maestre, C. Battilana, E. Calvo, M. Cerrada, M. Chamizo Llatas², N. Colino, B. De La Cruz, A. Delgado Peris, D. Domínguez Vázquez, C. Fernandez Bedoya, J.P. Fernández Ramos, A. Ferrando, J. Flix, M.C. Fouz, P. Garcia-Abia, O. Gonzalez Lopez, S. Goy Lopez, J.M. Hernandez, M.I. Josa, G. Merino, E. Navarro De Martino, J. Puerta Pelayo, A. Quintario Olmeda, I. Redondo, L. Romero, M.S. Soares, C. Willmott

Universidad Autónoma de Madrid, Madrid, Spain

C. Albajar, J.F. de Trocóniz

Universidad de Oviedo, Oviedo, Spain

H. Brun, J. Cuevas, J. Fernandez Menendez, S. Folgueras, I. Gonzalez Caballero, L. Lloret Iglesias

Instituto de Física de Cantabria (IFCA), CSIC-Universidad de Cantabria, Santander, Spain

J.A. Brochero Cifuentes, I.J. Cabrillo, A. Calderon, S.H. Chuang, J. Duarte Campderros, M. Fernandez, G. Gomez, J. Gonzalez Sanchez, A. Graziano, A. Lopez Virto, J. Marco, R. Marco, C. Martinez Rivero, F. Matorras, F.J. Munoz Sanchez, J. Piedra Gomez, T. Rodrigo, A.Y. Rodríguez-Marrero, A. Ruiz-Jimeno, L. Scodellaro, I. Vila, R. Vilar Cortabitarte

CERN, European Organization for Nuclear Research, Geneva, Switzerland

D. Abbaneo, E. Auffray, G. Auzinger, M. Bachtis, P. Baillon, A.H. Ball, D. Barney, J. Bendavid, L. Benhabib, J.F. Benitez, C. Bernet⁸, G. Bianchi, P. Bloch, A. Bocci, A. Bonato, O. Bondu, C. Botta, H. Breuker, T. Camporesi, G. Cerminara, T. Christiansen, J.A. Coarasa Perez, S. Colafranceschi³⁵, M. D'Alfonso, D. d'Enterria, A. Dabrowski, A. David, F. De Guio, A. De Roeck, S. De Visscher, S. Di Guida, M. Dobson, N. Dupont-Sagorin, A. Elliott-Peisert, J. Eugster, G. Franzoni, W. Funk, M. Giffels, D. Gigi, K. Gill, M. Girone, M. Giunta, F. Glege, R. Gomez-Reino Garrido, S. Gowdy, R. Guida, J. Hammer, M. Hansen, P. Harris, A. Hinzmann, V. Innocente, P. Janot, E. Karavakis, K. Kousouris, K. Krajczar, P. Lecoq, Y.-J. Lee, C. Lourenço, N. Magini, L. Malgeri, M. Mannelli, L. Masetti, F. Meijers, S. Mersi, E. Meschi, F. Moortgat, M. Mulders, P. Musella, L. Orsini, E. Palencia Cortezon, E. Perez, L. Perrozzi, A. Petrilli, G. Petrucciani, A. Pfeiffer, M. Pierini, M. Pimiä, D. Piparo, M. Plagge, A. Racz, W. Reece, G. Rolandi³⁶, M. Rovere, H. Sakulin, F. Santanastasio, C. Schäfer, C. Schwick, S. Sekmen,

A. Sharma, P. Siegrist, P. Silva, M. Simon, P. Sphicas³⁷, J. Steggemann, B. Stieger, M. Stoye, A. Tsiros, G.I. Veres²⁰, J.R. Vlimant, H.K. Wöhri, W.D. Zeuner

Paul Scherrer Institut, Villigen, Switzerland

W. Bertl, K. Deiters, W. Erdmann, K. Gabathuler, R. Horisberger, Q. Ingram, H.C. Kaestli, S. König, D. Kotlinski, U. Langenegger, D. Renker, T. Rohe

Institute for Particle Physics, ETH Zurich, Zurich, Switzerland

F. Bachmair, L. Bäni, L. Bianchini, P. Bortignon, M.A. Buchmann, B. Casal, N. Chanon, A. Deisher, G. Dissertori, M. Dittmar, M. Donegà, M. Dünser, P. Eller, C. Grab, D. Hits, W. Luster, B. Mangano, A.C. Marini, P. Martinez Ruiz del Arbol, D. Meister, N. Mohr, C. Nägeli³⁸, P. Nef, F. Nessi-Tedaldi, F. Pandolfi, L. Pape, F. Pauss, M. Peruzzi, M. Quitnat, F.J. Ronga, M. Rossini, L. Sala, A. Starodumov³⁹, M. Takahashi, L. Tauscher[†], K. Theofilatos, D. Treille, R. Wallny, H.A. Weber

Universität Zürich, Zurich, Switzerland

C. Amsler⁴⁰, V. Chiochia, A. De Cosa, C. Favaro, M. Ivova Rikova, B. Kilminster, B. Millan Mejias, J. Ngadiuba, P. Robmann, H. Snoek, S. Taroni, M. Verzetti, Y. Yang

National Central University, Chung-Li, Taiwan

M. Cardaci, K.H. Chen, C. Ferro, C.M. Kuo, S.W. Li, W. Lin, Y.J. Lu, R. Volpe, S.S. Yu

National Taiwan University (NTU), Taipei, Taiwan

P. Bartalini, P. Chang, Y.H. Chang, Y.W. Chang, Y. Chao, K.F. Chen, C. Dietz, U. Grundler, W.-S. Hou, Y. Hsiung, K.Y. Kao, Y.J. Lei, Y.F. Liu, R.-S. Lu, D. Majumder, E. Petrakou, X. Shi, J.G. Shiu, Y.M. Tzeng, M. Wang, R. Wilken

Chulalongkorn University, Bangkok, Thailand

B. Asavapibhop, N. Suwonjandee

Cukurova University, Adana, Turkey

A. Adiguzel, M.N. Bakirci⁴¹, S. Cerci⁴², C. Dozen, I. Dumanoglu, E. Eskut, S. Girgis, G. Gokbulut, E. Gurpinar, I. Hos, E.E. Kangal, A. Kayis Topaksu, G. Onengut⁴³, K. Ozdemir, S. Ozturk⁴¹, A. Polatoz, K. Sogut⁴⁴, D. Sunar Cerci⁴², B. Tali⁴², H. Topakli⁴¹, M. Vergili

Middle East Technical University, Physics Department, Ankara, Turkey

I.V. Akin, T. Aliev, B. Bilin, S. Bilmis, M. Deniz, H. Gamsizkan, A.M. Guler, G. Karapinar⁴⁵, K. Ocalan, A. Ozpineci, M. Serin, R. Sever, U.E. Surat, M. Yalvac, M. Zeyrek

Bogazici University, Istanbul, Turkey

E. Gülmez, B. Isildak⁴⁶, M. Kaya⁴⁷, O. Kaya⁴⁷, S. Ozkorucuklu⁴⁸, N. Sonmez⁴⁹

Istanbul Technical University, Istanbul, Turkey

H. Bahtiyar⁵⁰, E. Barlas, K. Cankocak, Y.O. Günaydin⁵¹, F.I. Vardarli, M. Yücel

National Scientific Center, Kharkov Institute of Physics and Technology, Kharkov, Ukraine

L. Levchuk, P. Sorokin

University of Bristol, Bristol, United Kingdom

J.J. Brooke, E. Clement, D. Cussans, H. Flacher, R. Frazier, J. Goldstein, M. Grimes, G.P. Heath, H.F. Heath, J. Jacob, L. Kreczko, C. Lucas, Z. Meng, S. Metson, D.M. Newbold⁵², K. Nirunpong, S. Paramesvaran, A. Poll, S. Senkin, V.J. Smith, T. Williams

Rutherford Appleton Laboratory, Didcot, United Kingdom

K.W. Bell, A. Belyaev⁵³, C. Brew, R.M. Brown, D.J.A. Cockerill, J.A. Coughlan, K. Harder,

S. Harper, J. Ilic, E. Olaiya, D. Petyt, C.H. Shepherd-Themistocleous, A. Thea, I.R. Tomalin, W.J. Womersley, S.D. Worm

Imperial College, London, United Kingdom

M. Baber, R. Bainbridge, O. Buchmuller, D. Burton, D. Colling, N. Cripps, M. Cutajar, P. Dauncey, G. Davies, M. Della Negra, W. Ferguson, J. Fulcher, D. Futyan, A. Gilbert, A. Guneratne Bryer, G. Hall, Z. Hatherell, J. Hays, G. Iles, M. Jarvis, G. Karapostoli, M. Kenzie, R. Lane, R. Lucas⁵², L. Lyons, A.-M. Magnan, J. Marrouche, B. Mathias, R. Nandi, J. Nash, A. Nikitenko³⁹, J. Pela, M. Pesaresi, K. Petridis, M. Pioppi⁵⁴, D.M. Raymond, S. Rogerson, A. Rose, C. Seez, P. Sharp[†], A. Sparrow, A. Tapper, M. Vazquez Acosta, T. Virdee, S. Wakefield, N. Wardle

Brunel University, Uxbridge, United Kingdom

J.E. Cole, P.R. Hobson, A. Khan, P. Kyberd, D. Leggat, D. Leslie, W. Martin, I.D. Reid, P. Symonds, L. Teodorescu, M. Turner

Baylor University, Waco, USA

J. Dittmann, K. Hatakeyama, A. Kasmi, H. Liu, T. Scarborough

The University of Alabama, Tuscaloosa, USA

O. Charaf, S.I. Cooper, C. Henderson, P. Rumerio

Boston University, Boston, USA

A. Avetisyan, T. Bose, C. Fantasia, A. Heister, P. Lawson, D. Lazic, J. Rohlf, D. Sperka, J. St. John, L. Sulak

Brown University, Providence, USA

J. Alimena, S. Bhattacharya, G. Christopher, D. Cutts, Z. Demiragli, A. Ferapontov, A. Garabedian, U. Heintz, S. Jabeen, G. Kukartsev, E. Laird, G. Landsberg, M. Luk, M. Narain, M. Segala, T. Sinthuprasith, T. Speer

University of California, Davis, Davis, USA

R. Breedon, G. Breto, M. Calderon De La Barca Sanchez, S. Chauhan, M. Chertok, J. Conway, R. Conway, P.T. Cox, R. Erbacher, M. Gardner, W. Ko, A. Kopecky, R. Lander, T. Miceli, D. Pellett, J. Pilot, F. Ricci-Tam, B. Rutherford, M. Searle, S. Shalhout, J. Smith, M. Squires, M. Tripathi, S. Wilbur, R. Yohay

University of California, Los Angeles, USA

V. Andreev, D. Cline, R. Cousins, S. Erhan, P. Everaerts, C. Farrell, M. Felcini, J. Hauser, M. Ignatenko, C. Jarvis, G. Rakness, P. Schlein[†], E. Takasugi, V. Valuev, M. Weber

University of California, Riverside, Riverside, USA

J. Babb, R. Clare, J. Ellison, J.W. Gary, G. Hanson, J. Heilman, P. Jandir, F. Lacroix, H. Liu, O.R. Long, A. Luthra, M. Malberti, H. Nguyen, A. Shrinivas, J. Sturdy, S. Sumowidagdo, S. Wimpenny

University of California, San Diego, La Jolla, USA

W. Andrews, J.G. Branson, G.B. Cerati, S. Cittolin, R.T. D'Agnolo, D. Evans, A. Holzner, R. Kelley, D. Kovalskyi, M. Lebourgeois, J. Letts, I. Macneill, S. Padhi, C. Palmer, M. Pieri, M. Sani, V. Sharma, S. Simon, E. Sudano, M. Tadel, Y. Tu, A. Vartak, S. Wasserbaech⁵⁵, F. Wirthwein, A. Yagil, J. Yoo

University of California, Santa Barbara, Santa Barbara, USA

D. Barge, C. Campagnari, T. Danielson, K. Flowers, P. Geffert, C. George, F. Golf, J. Incandela,

C. Justus, R. Magaña Villalba, N. Mccoll, V. Pavlunin, J. Richman, R. Rossin, D. Stuart, W. To, C. West

California Institute of Technology, Pasadena, USA

A. Apresyan, A. Bornheim, J. Bunn, Y. Chen, E. Di Marco, J. Duarte, D. Kcira, Y. Ma, A. Mott, H.B. Newman, C. Pena, C. Rogan, M. Spiropulu, V. Timciuc, R. Wilkinson, S. Xie, R.Y. Zhu

Carnegie Mellon University, Pittsburgh, USA

V. Azzolini, A. Calamba, R. Carroll, T. Ferguson, Y. Iiyama, D.W. Jang, M. Paulini, J. Russ, H. Vogel, I. Vorobiev

University of Colorado at Boulder, Boulder, USA

J.P. Cumalat, B.R. Drell, W.T. Ford, A. Gaz, E. Luiggi Lopez, U. Nauenberg, J.G. Smith, K. Stenson, K.A. Ulmer, S.R. Wagner

Cornell University, Ithaca, USA

J. Alexander, A. Chatterjee, N. Eggert, L.K. Gibbons, W. Hopkins, A. Khukhunaishvili, B. Kreis, N. Mirman, G. Nicolas Kaufman, J.R. Patterson, A. Ryd, E. Salvati, W. Sun, W.D. Teo, J. Thom, J. Thompson, J. Tucker, Y. Weng, L. Winstrom, P. Wittich

Fairfield University, Fairfield, USA

D. Winn

Fermi National Accelerator Laboratory, Batavia, USA

S. Abdullin, M. Albrow, J. Anderson, G. Apollinari, L.A.T. Bauerdick, A. Beretvas, J. Berryhill, P.C. Bhat, K. Burkett, J.N. Butler, V. Chetluru, H.W.K. Cheung, F. Chlebana, S. Cihangir, V.D. Elvira, I. Fisk, J. Freeman, Y. Gao, E. Gottschalk, L. Gray, D. Green, O. Gutsche, D. Hare, R.M. Harris, J. Hirschauer, B. Hooberman, S. Jindariani, M. Johnson, U. Joshi, K. KAADZE, B. Klima, S. Kwan, J. Linacre, D. Lincoln, R. Lipton, J. Lykken, K. Maeshima, J.M. Marraffino, V.I. Martinez Outschoorn, S. Maruyama, D. Mason, P. McBride, K. Mishra, S. Mrenna, Y. Musienko⁵⁶, S. Nahn, C. Newman-Holmes, V. O'Dell, O. Prokofyev, N. Ratnikova, E. Sexton-Kennedy, S. Sharma, W.J. Spalding, L. Spiegel, L. Taylor, S. Tkaczyk, N.V. Tran, L. Uplegger, E.W. Vaandering, R. Vidal, J. Whitmore, W. Wu, F. Yang, J.C. Yun

University of Florida, Gainesville, USA

D. Acosta, P. Avery, D. Bourilkov, T. Cheng, S. Das, M. De Gruttola, G.P. Di Giovanni, D. Dobur, R.D. Field, M. Fisher, Y. Fu, I.K. Furic, J. Hugon, B. Kim, J. Konigsberg, A. Korytov, A. Kropivnitskaya, T. Kypreos, J.F. Low, K. Matchev, P. Milenov⁵⁷, G. Mitselmakher, L. Muniz, A. Rinkevicius, L. Shchutska, N. Skhirtladze, M. Snowball, J. Yelton, M. Zakaria

Florida International University, Miami, USA

V. Gaultney, S. Hewamanage, S. Linn, P. Markowitz, G. Martinez, J.L. Rodriguez

Florida State University, Tallahassee, USA

T. Adams, A. Askew, J. Bochenek, J. Chen, B. Diamond, J. Haas, S. Hagopian, V. Hagopian, K.F. Johnson, H. Prosper, V. Veeraraghavan, M. Weinberg

Florida Institute of Technology, Melbourne, USA

M.M. Baarmand, B. Dorney, M. Hohlmann, H. Kalakhety, F. Yumiceva

University of Illinois at Chicago (UIC), Chicago, USA

M.R. Adams, L. Apanasevich, V.E. Bazterra, R.R. Betts, I. Bucinskaite, R. Cavanaugh, O. Evdokimov, L. Gauthier, C.E. Gerber, D.J. Hofman, S. Khalatyan, P. Kurt, D.H. Moon, C. O'Brien, C. Silkworth, P. Turner, N. Varelas

The University of Iowa, Iowa City, USA

U. Akgun, E.A. Albayrak⁵⁰, B. Bilki⁵⁸, W. Clarida, K. Dilsiz, F. Duru, J.-P. Merlo, H. Mermerkaya⁵⁹, A. Mestvirishvili, A. Moeller, J. Nachtman, H. Ogul, Y. Onel, F. Ozok⁵⁰, S. Sen, P. Tan, E. Tiras, J. Wetzel, T. Yetkin⁶⁰, K. Yi

Johns Hopkins University, Baltimore, USA

B.A. Barnett, B. Blumenfeld, S. Bolognesi, D. Fehling, A.V. Gritsan, P. Maksimovic, C. Martin, M. Swartz, A. Whitbeck

The University of Kansas, Lawrence, USA

P. Baringer, A. Bean, G. Benelli, R.P. Kenny III, M. Murray, D. Noonan, S. Sanders, J. Sekaric, R. Stringer, Q. Wang, J.S. Wood

Kansas State University, Manhattan, USA

A.F. Barfuss, I. Chakaberia, A. Ivanov, S. Khalil, M. Makouski, Y. Maravin, L.K. Saini, S. Shrestha, I. Svintradze

Lawrence Livermore National Laboratory, Livermore, USA

J. Gronberg, D. Lange, F. Rebassoo, D. Wright

University of Maryland, College Park, USA

A. Baden, B. Calvert, S.C. Eno, J.A. Gomez, N.J. Hadley, R.G. Kellogg, T. Kolberg, Y. Lu, M. Marionneau, A.C. Mignerey, K. Pedro, A. Skuja, J. Temple, M.B. Tonjes, S.C. Tonwar

Massachusetts Institute of Technology, Cambridge, USA

A. Apyan, G. Bauer, W. Busza, I.A. Cali, M. Chan, L. Di Matteo, V. Dutta, G. Gomez Ceballos, M. Goncharov, D. Gulhan, M. Klute, Y.S. Lai, A. Levin, P.D. Luckey, T. Ma, C. Paus, D. Ralph, C. Roland, G. Roland, G.S.F. Stephans, F. Stöckli, K. Sumorok, D. Velicanu, J. Veverka, B. Wyslouch, M. Yang, A.S. Yoon, M. Zanetti, V. Zhukova

University of Minnesota, Minneapolis, USA

B. Dahmes, A. De Benedetti, A. Gude, S.C. Kao, K. Klapoetke, Y. Kubota, J. Mans, N. Pastika, R. Rusack, A. Singovsky, N. Tambe, J. Turkewitz

University of Mississippi, Oxford, USA

J.G. Acosta, L.M. Cremaldi, R. Kroeger, S. Oliveros, L. Perera, R. Rahmat, D.A. Sanders, D. Summers

University of Nebraska-Lincoln, Lincoln, USA

E. Avdeeva, K. Bloom, S. Bose, D.R. Claes, A. Dominguez, R. Gonzalez Suarez, J. Keller, I. Kravchenko, J. Lazo-Flores, S. Malik, F. Meier, G.R. Snow

State University of New York at Buffalo, Buffalo, USA

J. Dolen, A. Godshalk, I. Iashvili, S. Jain, A. Kharchilava, A. Kumar, S. Rappoccio, Z. Wan

Northeastern University, Boston, USA

G. Alverson, E. Barberis, D. Baumgartel, M. Chasco, J. Haley, A. Massironi, D. Nash, T. Orimoto, D. Trocino, D. Wood, J. Zhang

Northwestern University, Evanston, USA

A. Anastassov, K.A. Hahn, A. Kubik, L. Lusito, N. Mucia, N. Odell, B. Pollack, A. Pozdnyakov, M. Schmitt, S. Stoynev, K. Sung, M. Velasco, S. Won

University of Notre Dame, Notre Dame, USA

D. Berry, A. Brinkerhoff, K.M. Chan, A. Drozdetskiy, M. Hildreth, C. Jessop, D.J. Karmgard,

J. Kolb, K. Lannon, W. Luo, S. Lynch, N. Marinelli, D.M. Morse, T. Pearson, M. Planer, R. Ruchti, J. Slaunwhite, N. Valls, M. Wayne, M. Wolf

The Ohio State University, Columbus, USA

L. Antonelli, B. Bylsma, L.S. Durkin, S. Flowers, C. Hill, R. Hughes, K. Kotov, T.Y. Ling, D. Puigh, M. Rodenburg, G. Smith, C. Vuosalo, B.L. Winer, H. Wolfe, H.W. Wulsin

Princeton University, Princeton, USA

E. Berry, P. Elmer, V. Halyo, P. Hebda, J. Hegeman, A. Hunt, P. Jindal, S.A. Koay, P. Lujan, D. Marlow, T. Medvedeva, M. Mooney, J. Olsen, P. Piroué, X. Quan, A. Raval, H. Saka, D. Stickland, C. Tully, J.S. Werner, S.C. Zenz, A. Zuranski

University of Puerto Rico, Mayaguez, USA

E. Brownson, A. Lopez, H. Mendez, J.E. Ramirez Vargas

Purdue University, West Lafayette, USA

E. Alagoz, D. Benedetti, G. Bolla, D. Bortoletto, M. De Mattia, A. Everett, Z. Hu, M. Jones, K. Jung, M. Kress, N. Leonardo, D. Lopes Pegna, V. Maroussov, P. Merkel, D.H. Miller, N. Neumeister, B.C. Radburn-Smith, I. Shipsey, D. Silvers, A. Svyatkovskiy, F. Wang, W. Xie, L. Xu, H.D. Yoo, J. Zablocki, Y. Zheng

Purdue University Calumet, Hammond, USA

N. Parashar

Rice University, Houston, USA

A. Adair, B. Akgun, K.M. Ecklund, F.J.M. Geurts, W. Li, B. Michlin, B.P. Padley, R. Redjimi, J. Roberts, J. Zabel

University of Rochester, Rochester, USA

B. Betchart, A. Bodek, R. Covarelli, P. de Barbaro, R. Demina, Y. Eshaq, T. Ferbel, A. Garcia-Bellido, P. Goldenzweig, J. Han, A. Harel, D.C. Miner, G. Petrillo, D. Vishnevskiy, M. Zielinski

The Rockefeller University, New York, USA

A. Bhatti, R. Ciesielski, L. Demortier, K. Goulios, G. Lungu, S. Malik, C. Mesropian

Rutgers, The State University of New Jersey, Piscataway, USA

S. Arora, A. Barker, J.P. Chou, C. Contreras-Campana, E. Contreras-Campana, D. Duggan, D. Ferencek, Y. Gershtein, R. Gray, E. Halkiadakis, D. Hidas, A. Lath, S. Panwalkar, M. Park, R. Patel, V. Rekovic, J. Robles, S. Salur, S. Schnetzer, C. Seitz, S. Somalwar, R. Stone, S. Thomas, P. Thomassen, M. Walker

University of Tennessee, Knoxville, USA

K. Rose, S. Spanier, Z.C. Yang, A. York

Texas A&M University, College Station, USA

O. Bouhali⁶¹, R. Eusebi, W. Flanagan, J. Gilmore, T. Kamon⁶², V. Khotilovich, V. Krutelyov, R. Montalvo, I. Osipenkov, Y. Pakhotin, A. Perloff, J. Roe, A. Safonov, T. Sakuma, I. Suarez, A. Tatarinov, D. Toback

Texas Tech University, Lubbock, USA

N. Akchurin, C. Cowden, J. Damgov, C. Dragoiu, P.R. Duderu, K. Kovitangoon, S. Kunori, S.W. Lee, T. Libeiro, I. Volobouev

Vanderbilt University, Nashville, USA

E. Appelt, A.G. Delannoy, S. Greene, A. Gurrola, W. Johns, C. Maguire, Y. Mao, A. Melo, M. Sharma, P. Sheldon, B. Snook, S. Tuo, J. Velkovska

University of Virginia, Charlottesville, USA

M.W. Arenton, S. Boutle, B. Cox, B. Francis, J. Goodell, R. Hirosky, A. Ledovskoy, C. Lin, C. Neu, J. Wood

Wayne State University, Detroit, USA

S. Gollapinni, R. Harr, P.E. Karchin, C. Kottachchi Kankanamge Don, P. Lamichhane, A. Sakharov

University of Wisconsin, Madison, USA

D.A. Belknap, L. Borrello, D. Carlsmith, M. Cepeda, S. Dasu, S. Duric, E. Friis, M. Grothe, R. Hall-Wilton, M. Herndon, A. Hervé, P. Klabbers, J. Klukas, A. Lanaro, R. Loveless, A. Mohapatra, I. Ojalvo, T. Perry, G.A. Pierro, G. Polese, I. Ross, T. Sarangi, A. Savin, W.H. Smith, J. Swanson

†: Deceased

- 1: Also at Vienna University of Technology, Vienna, Austria
- 2: Also at CERN, European Organization for Nuclear Research, Geneva, Switzerland
- 3: Also at Institut Pluridisciplinaire Hubert Curien, Université de Strasbourg, Université de Haute Alsace Mulhouse, CNRS/IN2P3, Strasbourg, France
- 4: Also at National Institute of Chemical Physics and Biophysics, Tallinn, Estonia
- 5: Also at Skobeltsyn Institute of Nuclear Physics, Lomonosov Moscow State University, Moscow, Russia
- 6: Also at Universidade Estadual de Campinas, Campinas, Brazil
- 7: Also at California Institute of Technology, Pasadena, USA
- 8: Also at Laboratoire Leprince-Ringuet, Ecole Polytechnique, IN2P3-CNRS, Palaiseau, France
- 9: Also at Zewail City of Science and Technology, Zewail, Egypt
- 10: Also at Suez Canal University, Suez, Egypt
- 11: Also at Cairo University, Cairo, Egypt
- 12: Also at Fayoum University, El-Fayoum, Egypt
- 13: Also at British University in Egypt, Cairo, Egypt
- 14: Now at Ain Shams University, Cairo, Egypt
- 15: Also at Université de Haute Alsace, Mulhouse, France
- 16: Also at Universidad de Antioquia, Medellin, Colombia
- 17: Also at Brandenburg University of Technology, Cottbus, Germany
- 18: Also at The University of Kansas, Lawrence, USA
- 19: Also at Institute of Nuclear Research ATOMKI, Debrecen, Hungary
- 20: Also at Eötvös Loránd University, Budapest, Hungary
- 21: Also at Tata Institute of Fundamental Research - EHEP, Mumbai, India
- 22: Also at Tata Institute of Fundamental Research - HECR, Mumbai, India
- 23: Now at King Abdulaziz University, Jeddah, Saudi Arabia
- 24: Also at University of Visva-Bharati, Santiniketan, India
- 25: Also at University of Ruhuna, Matara, Sri Lanka
- 26: Also at Isfahan University of Technology, Isfahan, Iran
- 27: Also at Sharif University of Technology, Tehran, Iran
- 28: Also at Plasma Physics Research Center, Science and Research Branch, Islamic Azad University, Tehran, Iran
- 29: Also at Università degli Studi di Siena, Siena, Italy
- 30: Also at Centre National de la Recherche Scientifique (CNRS) - IN2P3, Paris, France
- 31: Also at Purdue University, West Lafayette, USA
- 32: Also at Universidad Michoacana de San Nicolas de Hidalgo, Morelia, Mexico
- 33: Also at National Centre for Nuclear Research, Swierk, Poland

-
- 34: Also at Faculty of Physics, University of Belgrade, Belgrade, Serbia
 - 35: Also at Facoltà Ingegneria, Università di Roma, Roma, Italy
 - 36: Also at Scuola Normale e Sezione dell'INFN, Pisa, Italy
 - 37: Also at University of Athens, Athens, Greece
 - 38: Also at Paul Scherrer Institut, Villigen, Switzerland
 - 39: Also at Institute for Theoretical and Experimental Physics, Moscow, Russia
 - 40: Also at Albert Einstein Center for Fundamental Physics, Bern, Switzerland
 - 41: Also at Gaziosmanpasa University, Tokat, Turkey
 - 42: Also at Adiyaman University, Adiyaman, Turkey
 - 43: Also at Cag University, Mersin, Turkey
 - 44: Also at Mersin University, Mersin, Turkey
 - 45: Also at Izmir Institute of Technology, Izmir, Turkey
 - 46: Also at Ozyegin University, Istanbul, Turkey
 - 47: Also at Kafkas University, Kars, Turkey
 - 48: Also at Suleyman Demirel University, Isparta, Turkey
 - 49: Also at Ege University, Izmir, Turkey
 - 50: Also at Mimar Sinan University, Istanbul, Istanbul, Turkey
 - 51: Also at Kahramanmaras Sütcü Imam University, Kahramanmaras, Turkey
 - 52: Also at Rutherford Appleton Laboratory, Didcot, United Kingdom
 - 53: Also at School of Physics and Astronomy, University of Southampton, Southampton, United Kingdom
 - 54: Also at INFN Sezione di Perugia; Università di Perugia, Perugia, Italy
 - 55: Also at Utah Valley University, Orem, USA
 - 56: Also at Institute for Nuclear Research, Moscow, Russia
 - 57: Also at University of Belgrade, Faculty of Physics and Vinca Institute of Nuclear Sciences, Belgrade, Serbia
 - 58: Also at Argonne National Laboratory, Argonne, USA
 - 59: Also at Erzincan University, Erzincan, Turkey
 - 60: Also at Yildiz Technical University, Istanbul, Turkey
 - 61: Also at Texas A&M University at Qatar, Doha, Qatar
 - 62: Also at Kyungpook National University, Daegu, Korea